University of Zurich

University Hospital Zurich

Division of Internal Medicine

Supervisors

PD Dr. med. Florence Vallelian

Professor Dr. med. Dominik Schaer

Heme drives adaptive hypoinflammation in endothelial cells

Master thesis

Submitted to the Faculty of Sciences of the University of Zurich
in partial fulfilment of the requirements for the degree of Master
of Science in Medical Biology

Presented by

Dr. med. Kristyna Valkova
from Wädenswil ZH, Switzerland

Approved by

Prof. Dr. med. vet. Hanspeter Nägeli

Institute of Veterinary Pharmacology and Toxicology

University of Zurich

Zurich, January 2018

Table of contents

1 Abstract

Heme is a prosthetic group of oxygen carrier hemoglobin (Hb). During hemolytic conditions, such as sickle cell disease or malaria, heme can be released from cell-free Hb triggering toxicity through oxidative reactions. The role of heme in inflammatory processes has been extensively studied but remains not completely elucidated. Although activation of TLR4 and downstream inflammatory signaling pathways can be triggered by free heme, heme-catabolism through hemoxygenase 1 (Hmox-1) has been reported to downregulate some components of inflammation and immunity. In our laboratory, we could demonstrate that heme does not induce inflammation, suggesting that previous reports of pro-inflammatory heme-activity might have been influenced by the difficult biophysical properties of purified (protein-free) heme. In contrast, we have identified heme as a potent suppressor of inflammation in macrophages. Vascular endothelial cells, as sentinels for homeostasis in the blood stream, are among the first cells exposed to cell-free Hb and heme during hemolytic diseases.

To define the role of heme in the endothelial cell inflammatory response, we performed a number of in vitro and in vivo studies. In vitro, heme-treated endothelial cells were stimulated by IL-1β. In vivo, heme-treated mice were challenged with lipopolysaccharide (LPS) or with an agonistic anti-CD40 antibody, which induces a systemic inflammatory response with necrotizing hepatitis.

In the first part of the present study, we found that heme treatment suppresses the inflammatory signaling to IL-1β in human umbilical vein endothelial cells (HUVEC). The most interesting finding was that heme challenge suppresses the expression of the adhesion molecule VCAM-1, causing decreasing monocyte adhesion. Along the same line, in vivo heme challenge blunts the endothelial response in the context of a LPS-induced systemic inflammatory response syndrome. In a murine model of anti-CD40-induced necroinflammatory liver disease, heme-treatment rescues almost completely the phenotype of the disease.

In the second part of the study, we dissected the possible mechanisms for heme-induced hypoinflammation. Using a Hmox-1 knock-out mouse model, we could demonstrate that the hypoinflammation was related to heme itself and not to Hmox-1 activity, the main enzyme of heme-breakdown. Further, we identified Nrf2 activation as a possible candidate for heme-induced hypo-inflammation in endothelial cells. The heme gene signature of HUVEC is dominated by the expression of Nrf2 target genes. The transcription factor Nrf2 is involved in upregulation of anti-oxidant genes upon increase of oxidative stress in the cell. Recently, Kobayashi et al. described a novel property of Nrf2 in suppression of pro-inflammatory NFκB response genes transcription in macrophages.

In conclusion, we demonstrated a novel anti-inflammatory effect of heme on endothelial cells and suggested the Nrf2 anti-inflammatory pathway as a possible mechanism involved in this process.

2 Abbreviations

ALT	alanine transaminase
APC	antigen presenting cells
Approx.	approximately
ARE	antioxidant response elements
AST	aspartate transaminase
BSA	bovine serum albumin
CD40	CD40 receptor
CD40L	CD40 ligand
CD	Cluster of Differentiation
CO	Carbon monoxide
CO_2	Carbon dioxide
Ct	Cycle threshold
ddH20	bidestillated water
EBM	Endothelial Basal Medium
ELISA	Enzyme-linked Immunosorbent Assay
FAM	5(6)-carboxyfluorescein
FBS	fetal bovine serum
Fig	figure
FACS	Fluorescent Activated Cell Sorting
GSR	glutathione-disulfide reductase
h	hour(s)
Hb-Hp	hemoglobin/haptoglobin complex
H&E staining	hematoxylin and eosin staining
Hmox-1	hemoxygenase 1

Hmox-1 ko	hemoxygenase 1 knock-out
IL-8	human Interleukin-8
HUVEC	Human Umbilical Vein Endothelial Cells
IL-1	Interleukin-1
INFγ	Interferon γ
ICAM-1	intercellular adhesion molecule-1
i.p.	intraperitoneal
keap-1	Kelch-like ECH-associated protein
LPS	Lipopolysaccharide
LuEC	Lung endothelial cells
min	minutes
NFκB	necrosis factor κB
NQO1	NAD(P)H dehydrogenase [quinone] 1
Nrf2	Nuclear factor erythroid-2-related factor 2
OCR	oxygen consumption rate
PAMPs	Pathogen-associated molecular patterns
PBMCs	Peripheral Blood Mononuclear Cells
PBS	phosphate Buffered Saline
PVDF	Polyvinylidene difluoride
RA839	Nrf2 activator
RBC	red blood cell
rpm	rounds per minutes
RT-qPCR	Real-time quantitative Polymerase chain reaction
s	second
SA-PE	streptavidine-phycoerythrin

SD	standard deviation
Scl7a11	Sodium-independent cystine-glutamate antiporter
SOD	Superoxide dismutase
TLR4	Toll-like receptor 4
TNFα	Tumor necrosis factor α
USA	United States of America
VCAM-1	Vascular cell adhesion protein-1, CD 106

3 Introduction

3.1 Hemolytic diseases

Intravascular hemolysis can occur in a variety of medical conditions, which share the common problem of accelerated erythrocyte destruction. Hemolytic diseases include congenital hemolytic anemias like hereditary spherocytosis or G6PD deficiency, hemoglobinopathies such as sickle cell disease or thalassemias, and a broad group of secondary hemolytic diseases including infectious diseases like malaria or physical stressors like artificial heart valves or extra-corporal circulation [2]. In all these conditions, red blood cells are lysed to an increased degree and release free hemoglobin (Hb) into the circulation.

3.2 Hemoglobin and its functions

Hb is a highly conserved molecule in diverse species and serves primary as oxygen (O_2) carrier and carbon dioxide (CO_2) remover in the circulation to secure efficient respiration. To fulfill this function, Hb needs to be inside of the erythrocytes. When erythrocytes are destroyed under physiological conditions, the released Hb enters the blood stream and is bound to its scavenger protein haptoglobin (Hp). In intravascular hemolysis, Hp can be quickly depleted and Hb can reveal its adverse effects. Firstly, Hb extravasates and causes nitric oxide (NO) depletion in vascular wall, leading to vasoconstriction and hence pulmonary and blood pressure increase, a major factor regarding the development of cardiovascular events in hemolytic diseases [3, 4]. Secondly, free Hb reacts with lipids or proteins in the blood stream and leads to the development of radical oxygen species (ROS) or oxidizes to Met-Hb. The oxidation of Hb leads to conformational changes in globin chains causing the release of its prosthetic group heme in the blood stream [5].

3.3 Heme and its structure

Heme belongs to a family of porphyrins, which play a crucial role in many essential processes like redox reactions or oxygen transport in almost all living organisms. Heme b, a prosthetic group of human Hb, consists of protoporphyrin IX with one central iron (Fe^{2+}) atom, which acts as acceptor and donator of oxygen (O_2) molecule and is therefore one of the most central molecules in human body. The oxygen carrier protein Hb consists of two dimers of α- and β-globin chains (α1β1 and α2β2) and four heme b prosthetic groups. Each heme b consists of four pyrrole rings, sharing a common central Fe^{2+} atom (Figure 1). The unique constellation of heme groups and globin chains allows cooperative binding and release of O_2 with increasing affinity from the first to the fourth O_2 binding, a main principle of oxygen transport in human body [1].

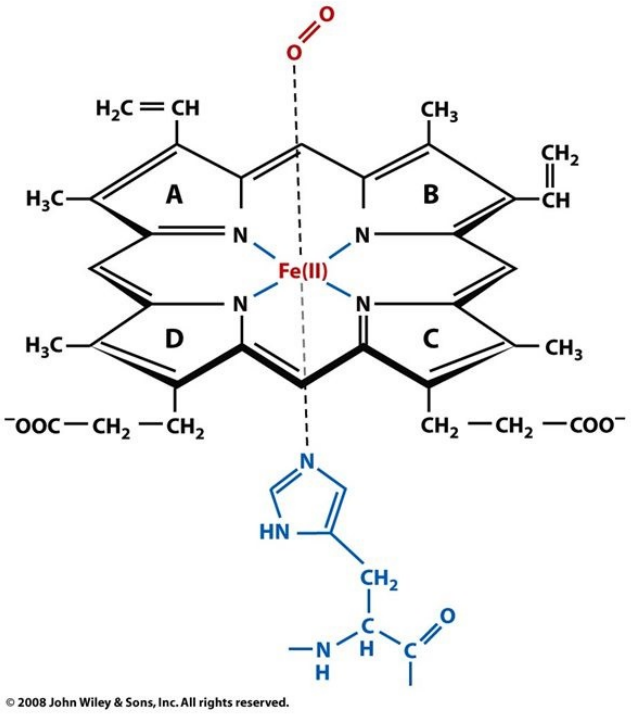

Figure 1: Oxygenated (Fe2+) form of heme [1]

A-D: four pyrrole rings, **Fe(II):** central iron atom with binding to O2 and protein chain

3.4 Heme and its functions

Because of its high oxidation potential, free heme contributes to oxidative stress by production of ROS and is thus thought to play a key role in Hb toxicity [6]. However, an elaborate scavenging system is protecting the vascular system from heme toxicity. When free heme enters plasma, it is bound with high affinity to its endogenous scavenger protein hemopexin or other hemoproteins and then degraded predominantly in the liver by the enzyme hemoxygenase-1 (Hmox-1) [5]. The anti-oxidative and anti-inflammatory protein Hmox-1 is the rate-limiting enzyme in heme breakdown and is present in all cell types. Hmox-1 catabolizes heme degradation to its products carbon monoxide (CO), biliverdin and iron, which are known for their anti-inflammatory properties [7, 8]. Besides its oxygen carrier function, heme acts as signaling molecule in extra- and intracellular responses by binding to several receptors, transcription factors and enzymes. Notably, heme is known to activate Toll-like receptor 4 (TLR4) and its downstream necrosis factor κB (NFκB) inflammatory signaling [9-11]. However, the question whether free heme is pro- or anti-inflammatory is still subject of debate. In our laboratory, we have demonstrated that heme does not induce inflammation [12]. This contradictory observation may be explained by the difficult biophysical properties of heme. Moreover, heme as a strongly lipophilic molecule is almost insoluble in aqueous environment and will under physiological conditions, as soon as released form Hb, immediately bind to other serum hemoproteins like hemopexin, or to lipoproteins, making unlikely that significant quantities of free monomeric heme can be present in the plasma [13]. Recent data from our laboratory identified heme as a potent suppressor of inflammation in macrophages (manuscript in preparation).

3.5 Endothelial cells and their function

Endothelial cells build the inner layer of blood vessels and play a key role in adjustment reactions of vascular system to changes in blood homeostasis, because of their crucial position between blood and surrounding tissue. The main functions of endothelial cells include their barrier function and their function as vasomotor regulators and initiators of the coagulation cascade after vascular injury [14]. Dysregulation of this delicate system can lead to thrombosis formation, thrombolysis impairment, vascular leakage and edema [14]. Furthermore, endothelial cells are capable to identify danger signals and hence to initiate immune system activation [14-16].

3.6 Inflammatory response in endothelial cells

Activation of endothelial cells and their role as sentinel cells in the bloodstream is a crucial mechanism for the immune system to fight infections. Endothelial cells show fast inflammatory response to presence of bacteria, viruses and foreign substances in blood stream. Different receptors on endothelial surface are involved in response to diverse pro-inflammatory stimuli. The direct activation of endothelial inflammatory response by pathogens in the bloodstream occurs via different TLR signaling [14]. For example, lipopolysaccharide (LPS), an archetypical representative of pro-inflammatory stimuli called Pathogen-Associated Molecular Patterns (PAMPs), is very efficiently recognized by a variety of cells including endothelial cells via their surface receptor TLR4 [17]. LPS/TLR4 binding initiates pro-inflammatory NFκB pathway activation, inducing a robust release of IL-6 and IL-8 [15] and upregulation of adhesion molecules such as Vascular Cell Adhesion Protein 1 (VCAM-1), Intercellular Adhesion Molecule 1 (ICAM-1) or E-selectin to facilitate leucocyte adherence and promote transendothelial migration [14, 16, 18]. Release of the chemokine IL-8 from activated endothelial cells acts as a strong promotor of monocyte adhesion to endothelial cells after cytokine activation [19]. Transcription factor NFκB is a central element in cellular inflammatory response, which regulates transcriptional upregulation of pro-inflammatory cytokines, chemokines and adhesion molecules [15]. A very common indirect activation of endothelial cells by LPS occurs via activation of innate immune cells, especially monocytes and granulocytes, and their release of

potent NFκB pathway chemokines TNFα and IL-1β, which trigger activation of endothelial cell inflammatory response [15, 20].

3.7 CD40 ligand-CD40 receptor signaling

Besides the classical LPS-induced, TLR4-dependent endothelial activation, CD40 receptor (CD40) represents a different pro-inflammatory signaling receptor. Yet, both receptors share a common NFkB end pathway [21].

CD40/CD40 ligand (CD40L) signaling is very well established in the context of adaptive immune response initiation as a secondary signal. The primary signal through activated antigen receptors on T- and B-lymphocytes is needed to start adaptive immune response, but rigorous control of this process is essential and so secondary signals from a variety of co-stimulatory receptors are involved in its regulation. Hereby, one of the most important co-stimulatory receptors is the CD40. CD40 is expressed on different antigen presenting cells (APC), including B-cells, monocytes and macrophages, but can also be found on endothelial, epithelial and some tumor cells, where it acts as a primary inflammatory receptor for innate immune response [22].

Endogenous CD40L is expressed in the organism mainly on activated CD4+ T-cells and binds to CD40 on the APC [23]. CD40/CD40L binding enhances cellular innate immune responses like chemokine and cytokine release from macrophages, or expression of adhesion molecules on endothelial cells. In the cells of innate immunity, CD40/CD40L binding initiates their inflammatory mediator production and release. Imbalance in this interaction may lead to development of autoimmune or inflammatory diseases [23]. Activation of CD40 was recently shown to play a central role in inflammatory liver disease including allograft rejection and viral hepatitis [21].

A model of necroinflammatory liver disease induced by the application of an anti-CD40 antibody, which mimics the effect of endogenous CD40L, was previously described and studied in the mouse [24, 25]. Anti-CD40L-dependent macrophage activation, leading to elevation of inflammatory cytokines like tumor necrosis factor-α (TNFα), was reported in this context [21].

3.8 Nrf2 and Nrf2/keap-1 pathway

Nuclear factor erythroid-2-related factor 2 (Nrf2) is the principal transcription factor that regulates expression of approximately 200 antioxidant genes upon oxidative or xenobiotic stress [26] [27]. Nrf2 dependent upregulation of anti-oxidant gene transcription leads to enhanced elimination of reactive oxygen species (ROS) in the cell.

In an unstressed cell, Nrf2 resides in the cytoplasm bound to its inhibitory protein Kelch-like ECH-associated protein (keap-1) and is degraded by E3 ubiquitin ligase in lysosomes. Upon activation through increased ROS, keap-1 dissociates from Nrf2 and the transcription factor is free to enter the nucleus and bind to the antioxidant response elements (ARE)-regions and start the transcription of its target genes [28-30]. The typical Nrf2 transcription modulation includes upregulation of ROS degradation enzymes like superoxide dismutase (SOD) or glutathione-disulfide reductase (GSR) and other typical Nrf2 gene targets like Hmox-1 hemoxygenase 1 (Hmox-1) or NAD(P)H dehydrogenase [quinone] 1 (NQO1) [31].

In the recent years, the role of Nrf2 in anti-inflammation drew increased attention in the research community. Nrf2 activation has been linked to transcriptional suppression of NFkB-dependent pro-inflammatory cytokines [9, 18], and this mechanism was connected to the Nrf2-dependent anti-oxidative upregulation of Hmox-1 [30], but the exact mechanism could not yet been completely unraveled.

Recently, Kobayashi et al. described Nrf2-dependent transcriptional inhibition of proinflammatory cytokine genes in macrophages, which appears to be independent of the classical Nrf2 anti-oxidative pathway driven by ROS [29]. They demonstrated that pro-inflammatory cytokines IL-1β and IL-6 have no ARE regions and no Nrf2 transcription factor binding sites in their promotor regions or in the proximity of their genes, hence an alternative Nrf2-dependent transcriptional regulation must exist. Further, they confirmed that Nrf2 suppresses upregulation of NFkB-dependent pro-inflammatory pathway, but they could show that NFkB binding to the regulatory regions of its

response genes is not disturbed [29]. In summary, the anti-inflammatory inhibiting effect on transcription of NfkB pathway genes and the anti-oxidative upregulatory effect on antioxidant genes may be two separate effects of Nrf2.

The importance of Nrf2 in the cellular anti-inflammatory processes was described in variety of diseases like multiple sclerosis (or its murine pendant experimental autoimmune encephalomyelitis), diabetes or autoimmunity [32-34]. Interestingly, the Nrf2 inducer Dimethylfumarate (Tecfidera®) has recently been established as a novel drug in multiple sclerosis therapy and is evaluated for use as an anti-inflammatory drug in other autoimmune diseases.

3.9 Hypothesis and aims

The overall aim of this project is to characterize the anti-inflammatory effects of heme and dissect its mechanistic pathway on endothelial cells.

Hypothesis

Heme treatment suppresses inflammatory responses of endothelial cells to typical inflammatory agonists in vitro and in vivo.

Aim 1

To characterize the effect of heme on endothelial cell activation and inflammation in human endothelial cells in vitro and in mouse models in vivo

Aim 2

Dissect the mechanistic pathway involved in the suppressive effect of heme on inflammatory responses of endothelial cells.

4 Material and Methods

4.1 Cell culture conditions and experimental treatment on HUVEC

Human umbilical vein endothelial cells (HUVEC, Lonza, Walkersville MD, USA) were cultured on rat tail collagen type I (Corning, Corning NY, USA) coated plates in Endothelial basal medium (EBM, Lonza) enriched with EGM SingleQuots (Lonza) containing human epidermal growth factor (hEGF), hydrocortisone, Gentamycin-1000, 2% fetal bovine serum (FBS) and ascorbic acid according to the supplement list given by the manufacturer. Cryopreserved cells were expanded until passage 3 and frozen back at -80°C with a supplement of DMSO as a cryopreservant. For experiments, cells were subsequently put back in the culture and used from passage 5 to 6. HUVEC were cultured under standard conditions at 37°C with 80% humidity under 5% CO2. Culture medium was changed every 48h. The experimental treatments were conducted on confluent layer of HUVEC. The standard treatment consisted of heme-albumin treatment in concentrations ranging from 0 to 160µM in the standard culture media for 4h followed by treatment with human inflammatory agonist Interleukin-1β (IL-1) at a standard working concentration of 100U/ml for 4h. After 8h of treatment, the cells were harvested for future analysis. Modifications to this standard treatment protocol are indicated in the corresponding method sections.

4.2 Heme-albumin preparation

A 4mM heme-albumin solution was prepared as follows: 65mg Hemin (Frontier Scientific, Inc., Logan, UT, USA) was dissolved in 10ml 100mM NaOH in a water bath at 37°C. After 10 min, 10ml of 20% human serum albumin (CSL Behring AG, Bern, Switzerland) were added and incubated at 37°C for 1h to enable the formation of heme-albumin. Next, thepH of the solution was adjusted to 7.45 using ortho-phosphoric acid and the solution was sterile-filtered (0.22µm). The 4mM heme-albumin solution was used within 24h for the experiments, diluted in the culture medium to the working concentrations indicated, or for i.p. injections in the mice.

4.3 RNA Isolation and quantitative Real time polymerase chain reaction

4.3.1 RNA Isolation

RNA was isolated using QIAgen RNAeasy Mini Kit (QIAgen, Hilden, Germany) according to the manufacturer's instructions including DNA digestion step. Shortly, confluent HUVEC on 6-well culture plates were lysed using RLT-Lysis buffer (QIAgen, Basel, Switzerland) containing 1% 2-Mercaptoethanol, collected to 1.5ml tubes and stored at -80°C. RNA was isolated and the quality and quantity was determined spectrophotometrically on the NanoDrop ND-1000® instrument. Total RNA was reverse transcribed to cDNA with TaqMan Reverse Transcription reagents (Applied Biosystems, Carlsbad CA, USA) on a Mastercycler gradient (Vaudaux-Eppendorf, Schoenenbuch, Switzerland) with the following cycle settings: 25°C for 10 minutes, 48°C for 30min and 95°C for 5min, followed by holding step at 4°C. The obtained cDNA was spectrophotometrically quantified and diluted to an approximate concentration of 300 ng/µl with RNAse free water.

4.3.2 RT-qPCR

Real-Time quantitative Polymerase Chain Reaction (RT-qPCR) was performed on the AB 7500 FAST-Real-Time PCR System (Applied Biosystems, Carlsbad CA, USA) using 2µl of cDNA, 10µl of TaqMan FAST Universal PCR Mastermix (2x) (Applied Biosystems, Carlsbad CA, USA), 7µl RNAse-free water, and 1µl primer following the TaqMan FAST Run method, which doesn't require an activation step

due to hot-start DNA polymerase. The RT-qPCR profile contains an initial denaturation step (20s at 95°C), followed by 40 cycles of alternate denaturation (3s at 95°C) and annealing/elongation (30s at 60°C).

Alternatively, the SYBR green qPCR method with 10 µl PowerSYBR green PCR Mastermix (Applied Biosystems, Carlsbad CA, USA), 7.2µl RNA-free water, 0.8µl primer mix and 2µl cDNA was applied on the same instrument with the following temperature profile: 20s at 50°C,10min at 95°C, 40 cycles of alternate denaturation (15s at 95°C) and annealing/elongation (60s at 60°C). Subsequently, the melting curve was determined and checked for unspecific amplification and primer-dimer building after each qPCR run.

Data were calculated as fold change in mRNA levels and normalized to the Ct (cycle threshold) values of the unregulated reference gene HPRT using the ΔΔCt method.

4.3.3 Primer design

Primers for the SYBR green method were designed with the Universal Probe Library Assay Design Center (Roche Lifescience software) and checked for quality with OligoAnalyzer3.1 (IIntegrated DNA Technologies) including matching temperature of forward and reverse primer, formation of primer dimers or hairpin structures. Selected primer pairs were ordered from Microsynth (Microsynth AG, Balgach, Switzerland). Human primers used for SYBR green amplification are listed in table 1. FAM (5(6)-carboxyfluorescein) primers for human and mouse genes were ordered online from Thermo Fisher (Thermo Fisher Scientific, Waltham MA, USA) and are listed in table 2 and 3.

Table 1: Primers to human genes for use in SYBR Green amplification

Gene	(5' - 3')	(3' - 5')
HPRT	TGACCTTGATTTATTTTGCAT	CGAGCAAGACGTTCAGTCCT
E-Selectin	TGGCAATGAAAAATTCTCAGTCA	TCAAGGCTAGAGCAGCTTTGG
IL-8	CCTTTCCACCCCAAATTTATCA	TGGTCCACTCTCAATCACTCTCAG
Hmox-1	AGGCCAAGACTGCGTTCCT	GGTGTCATGGGTCAGCAGC

NQO1	GGGATCCACGGGGACATGAATG	ATTTGAATTCGGGCGTCTGCTG
SLC7A11	CCATGAACGGTGGTGTGTT	GACCCTCTCGAGACGCAAC
PTGS2	CTTCACGCATCAGTTTTTCAAG	TCACCGTAAATATGATTTAAGTCCAC
VCAM-1	TGCACAGTGACTTGTGGACAT	CCACTCATCTCGATTTCTGGA
GSR	ATGATCAGCACCAACTGCAC	CGACAAAGTCTTTTTAACCTCCTT

Table 2: FAM Primers to human genes

Gene	Order Number
HPRT	Hs02800695_m1
ICAM1	Hs00164932_m1
E-Selectin	Hs00950401_m1
Hmox-1	Hs01110250_m1
VCAM-1	Hs01003372_m1
NQO1	Hs00168547_m1
SLC7A11	Hs00921938_m1

Table 3: FAM Primers to murine genes

Gene	Order Number
HPRT	Mm01545399_m1
ICAM1	Mm00516023_m1
Hmox-1	Mm00516005_m1
VCAM-1	Mm01320970_m1
NQO1	Mm01253561_m1
SLC7A11	Mm00442530_m1

4.4 VCAM-1 In-Cell Western Immunofluorescent Assay

In-Cell Western Immunofluorescent Assay combines the techniques of Western Blotting and Enzyme-linked Immunosorbent Assay (ELISA) and enables measurement of cell surface protein levels directly in fixed cultured cells [35][36].

Cellular VCAM-1 was measured using the in cell method as follows: HUVEC were cultured directly in a 96-well plate precoated with rat tail collagen type I until they reached over 90% confluency. Cells were pretreated 4h with 0, 80 or 160µM heme-albumin, subsequently stimulated with standard concentration of 100U/ml IL-1 for additional 4h. Supernatants were collected and cells were immediately fixed with 3.7% formaldehyde directly in the plate for 20 min. The cells were washed and permeabilized with 0.1% Triton-X-PBS solution and then blocked with LI-COR Odyssey Blocking Buffer (LI-COR Biotechnology, Lincoln NE, USA). Primary goat-anti-hVCAM-1 (R&D Systems, Inc., Minneapolis MN, USA) was diluted 1:8000 in LI-COR Odyssey Blocking Buffer and added to the cells for 1h. After another washing step, the cells were incubated with the secondary antibody donkey anti-goat IRDye® 800CW 1 µg/ml (LI-COR) and, at the same time, with the far-red fluorescent live-cell permanent DNA Dye DRAQ5™ (0.5 µM; Cell Signaling Technology Inc., Danvers MA, USA) for 1h. After final washing, the immunofluorescence was immediately measured with an Odyssey infrared imager (LI-COR) at 700nm for the red live-cell DNA stain DRAG5™ and at 800nm for the VCAM-1 green signal, simultaneously. The data were analyzed with Odyssey software (LI-COR).

4.5 IL-8 Immunoassay

Bio-Plex Pro® Assay technology works similar to a combination of sandwich enzyme-linked immunosorbent assay (ELISA) and FACS analysis [37]. Due to a special detection system similar to flow cytometry (FACS), this technology enables to detect multiple molecules of interest and determine their concentrations in one experimental plate.

Bio-Plex Pro® Assay (Bio-Rad Laboratories AG, Cressier, Switzerland) was carried out exactly according to manufacturer's instructions. Shortly, culture supernatants from the above described

VCAM-1 In cell Assay were diluted 1:4 in assay buffer and then added to 96-well plates containing fluorescent dyed beads coupled to human IL-8-antibody. In second step, streptavidine-phycoerythrin (SA-PE) marked detection complex was added and after an incubation and a washing step, the plates were directly read on a Bio-Plex 200 system (Bio-Rad) and analyzed using Bio-Plex Data Pro software (Bio-Rad).

4.6 Monocyte adhesion Assay

HUVEC were cultured in 96-well plates to >90% confluency. The confluent cells were prestimulated with heme-albumin (0,80,160µM) for 4h and then treated with human IL-1β (100U/ml) for 1h. Human monocytes were isolated from peripheral blood of healthy volunteers obtained from the Swiss Red Cross Blood Bank according to our monocyte isolation protocol as described previously [38, 39]. The human blood-derived monocytes were fluorescence labelled with Calcein (R&D Systems) and then prestimulated for 1h with LPS (1µg/ml). In the next step, 40'000 activated monocytes were added per well of confluent HUVECs and incubated for 30min at 37°C. Then, the plates were washed with PBS to remove non-adherent cells. Fluorescence of adherent monocytes was quantified at 485nm (excitation) and 520nm (emission) with the Tecan infinite M200 pro instrument and Tecan i-control I.II software (Tecan Group Ltd., Männedorf, Switzerland).[40]

4.7 Electric cell impedance measurement

ECIS® (Electric Cell-substrate Impedance Sensing) is a real-time method, which records changes in trans-endothelial electric resistance of endothelial monolayer under standardized conditions continuously over time. Therefore, cell growth and changes in barrier function and cell permeability of endothelial cells in response to experimental treatments can be studied by determination of impedance over time. Impedance is the equivalent of resistance in settings using alternating instead of direct current. We recorded real-time endothelial barrier function changes using ECIS Zθ system and ECIS Software v.1.2.70.1 PC (Applied BioPhysics, Troy NY, USA) according to our protocol as described in [41].

Shortly, ECIS 8W10E+ chamber arrays were equilibrated with DMEM (Gibco, Carlsbad CA, USA) medium without serum for 4h and coated with rat tail collagen type I (Corning) for 2 h. In a next step, 70'000 HUVEC in standard culture medium were added to each chamber well, put in incubator (37°C, 80% humidity, 5% CO2), and the experiment was started immediately. Our impedance measurement in ohms (Ω) was run at a frequency of 16kHz in ECIS 8W10E+ arrays containing 40 electrodes per each of its 8 wells. The cell monolayer impedance is at the same time measured at 40 different locations in each well and averaged to mean impedance for every time point. The cells were cultured until a dense monolayer of confluent cells was reached. During the growth of the cells on the gold electrodes, a steadily increase of impedance is observed. As the cells come to confluency, the impedance reaches a stable plateau and the experimental treatments can be started.[4] HUVEC were treated with 0, 80,160 and 320µM heme-albumin in culture medium and the changes in impedance over time were recorded for the following 12h.

4.8 Extracellular Flux Assay

Extracellular Flux Assay is a noninvasive method to measure effects of experimental treatments on mitochondrial function on living cells.[42]. During the measurement 3 different compounds, namely oligomycin, FCCP and rotenone/antimycin A are injected into the experimental wells. These compounds are selective inhibitors of mitochondrial complexes V (oligomycin) and complexes I/III(rotenone/antimycin A), and FCCP is a disruptor of H+-gradient of the mitochondrial membrane. With selective inhibition of these complexes, ATP-linked respiration, maximal respiration, and nonmitochondrial respiration of the cells, are determined (figure 2) [43]. As read-outs for mitochondrial respiration and glycolysis rate, changes in maximal oxygen consumption rate (OCR) and extracellular acidification rate (ECAR) are measured after addition of experimental treatments. Moreover, changes in mitochondrial function of the cells are sensitive markers for cell survival and cell death.

We used Agilent Seahorse XFp Cell Mito Stress Test Kit (Agilent Technologies, Santa Clara CA, USA) following strictly the protocol given by the manufacturer. In short, we seeded 40'000 HUVEC

cells/well directly on XFp cell culture miniplates (Agilent Technologies) and cultured them for 24h at 37°C under standard conditions. After 24h half of the medium was removed and replaced by experimental treatment medium with different concentrations of heme-albumin (0, 80,160µM) for 6h. Untreated samples and blank wells in duplicates were included as controls. After a washing step and 1h incubation without treatment, the mitochondrial function was determined running the Mito stress test seahorse program on the Seahorse XFp Analyzer (Agilent Technologies). Data show the difference in OCR and ECAR over time between control and heme-albumin treated samples.

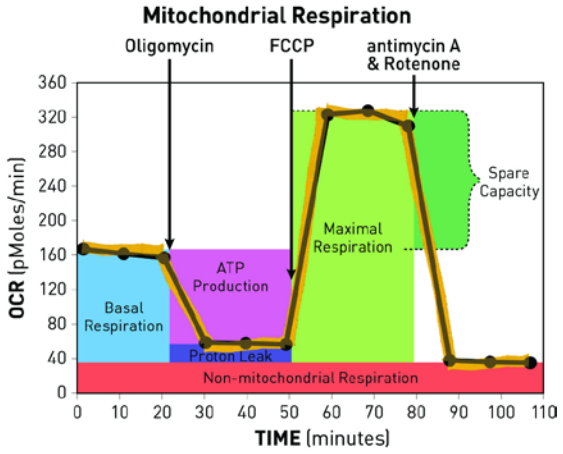

Figure 2: Principle of mitochondrial respiration measurement with Agilent Seahorse XFp Cell Mito Stress Test Kit [44]

4.9 Nrf2 Translocation Assay

HUVEC were cultured in 150mm × 25mm rat tail collagen precoated dishes as described before and culture medium was changed 24h before the experiment. Confluent HUVEC were treated with 0,80,160µM heme-albumin or 20µM RA839 (commercial Nrf2 activator) for 6h and cytoplasmic and nuclear protein fractions were subsequently isolated with Nuclear Extract Kit (active motif, Carlsbad CA, USA) according to the manufacturer's instructions. Briefly, the cells were washed with ice-cold PBS containing phosphatase inhibitor and removed from the plates by gently scraping. After a centrifugation step at 200xg for 5min at 4°C, the cell pellet was resuspended in 1xHypotonic Buffer and incubated for 15 min on ice. Then, detergent was added to the solution and the cell lysates were

vortexed for 10s at the highest setting. Efficiency of the lysis was controlled by comparison of 10µl before- and after-lysis samples by phase-contrast microscopy. To separate the nuclear fraction, samples were centrifuged at high rate (14000xg-30s-4°C) and supernatants containing cytoplasmic fractions were transferred to separate tubes and stored at -80°C.

The remaining nuclear pellets were resuspended in complete lysis buffer. 2.5µl detergent were added to solubilize membrane-associated nuclear proteins and the samples were mixed by vortexing at highest rate for 30s and incubated for 30min on a rocking platform at 150rpm and 4°C.

After another vortexing and centrifugation step (14000xg-10min-4°C), supernatants containing nuclear fractions were transferred to a new tube and stored at -80°C.

Protein concentrations of both cytoplasmatic and nucleic fractions were measured with Bradford Assay. Complete Lysis Buffer 1:50 dilution was used as a blank.

Samples were mixed with 2x Laemmli buffer, heated at 95°C for 5min and then separated on a polyacrylamide gel (Criterion™ TGX Stain-Free™ Precast Gel, BioRad, Hercules CA, USA) under following running conditions: 200V, 35-55mA, 35min. Precision Plus Protein All Blue Prestained Protein Standard (Bio-Rad) was run simultaneously as a control. After electrophoresis, proteins were transferred to a PVDF (Polyvinylidene difluoride) membrane (Thermo Scientific, USA) in a wet electrotransfer chamber (Criterion™ Blotter, BioRad) under constant voltage (100V) for 30min. Thereafter, the membrane was blocked with 10% goat serum and 1% bovine serum albumin for 1h and then cut at 75kb. The upper part of the membrane was incubated with primary antibody against human Nrf2 (Active motif), diluted 1:1000 in 1%Tween-PBS at 4°C overnight. The lower part of the membrane was incubated at 4°C overnight in primary antibody against human β-actin (1:2000 dilution in 1% Tween-PBS, Sigma) used as a loading control.

After washing with 1%Tween-PBS, the upper part of the membrane was incubated in anti-rabbit-horseradish peroxidase antibody (1:4000 dilution), and the lower part in Alexa Fluor® 488 goat anti-mouse IgG at room temperature for 1h.

After final washing, chemiluminescence detection for the upper part of the membrane was performed using Supersignal® West Femto Maximum Sensitivity Substrate (Thermo Scientific) and the membrane was immediately analyzed on a ChemiDoc MP Imaging system with Image Lab 5.2.1 software (Bio-Rad). The lower part of the membrane was analyzed in the ChemiDoc MP Imaging system in fluorescence detection mode, detecting immunofluorescence at 488nm.

4.10 In vivo experiment heme ± LPS in mice

We designed an in vivo experimental setup using wild type and Hmox-1 knockout mice to elucidate the role of heme on endothelial cell activation in vivo and the role of Hmox-1 in this process. In the UBC cre-ERT2 +/- Hmox-1 flox/flox mouse model, Cre recombinase is fused to estrogen receptor (ER) ligand-binding domain under the ubiquitary UBC promotor and is activated at a specific time point by addition of exogenous estrogen receptor ligand (in our case Tamoxifen) to the model system. Activated Cre recombinase cuts the DNA at lox marked sites, which flank the Hmox-1 alleles, and cause a removal of Hmox-1 from the DNA.

Wild-type C57BL/6J animals used in our experiments were obtained from Charles River (Wilmington, MA, USA). UBC cre-ERT2 +/- Hmox-1 flox/flox animals were bred in our facility, genotyped at birth and then at the age of 4 weeks treated on 5 following days with tamoxifen gavage (Sigma-Aldrich; 200g/kg body weight) to activate cre recombinase and obtain hmox1 knockout animals. The animals were re-genotyped 4 weeks after tamoxifen treatment and Hmox-1 knock-out animals were subsequently used within 1 week for the experiment. The animals were treated overnight with heme-albumin 100µmol/kg body weight (wild-type animals) or 50 µmol/kg body weight (Hmox-1 knockout animals) intraperitonealy (i.p.), following 4h treatment with LPS 0.5mg/kg body weight i.p. as an TLR4 agonist. The protocol of our experiment was proved by the Veterinary Office of the canton of Zurich under the license number 078/2016. All animals were housed at the Laboratory Animal Services Center (LASC) of the University of Zurich and were treated according to guidelines of the Swiss Federal Veterinary Office.

4.11 Murine lung cell isolation

Lung cells from heme-albumin and/or LPS treated mice were isolated for further analysis by flow cytometry and RT-qPCR. The mice were sacrificed by cervical dislocation. Lungs were flushed with PBS by right-ventricle perfusion of the beating heart to eliminate blood cells from the lung circulation. Lung lobes were removed separately, washed with ice-cold PBS and lung digestion was promptly started using the Lung Dissociation Kit (Miltenyi Biotec, Bergisch Gladbach, Germany) according to manufacturer's instructions. Lung lobes were put into digestion enzyme mix and placed in C Tubes (Miltenyi Biotec) on gentle MACS™ Octo Dissociator with Heaters (Miltenyi Biotec) for 30 min following the 37°C_LDK_1 program. After termination of the program, cell suspensions were filtered (70µm), washed with 2.5ml Buffer S and centrifuged at 300xg for 10min. Supernatant was discarded and cells were resuspended in 2 ml FACS Buffer containing 0.1%BSA. Lung cells were counted on a NucleoCounter® using a 10µl aliquot and processed immediately for further use in flow cytometry or FACS sorting.

4.12 Flow cytometry and FACS sorting of murine lung endothelial cells

4.12.1 Flow cytometry

Flow cytometry experiments were performed to characterize the lung endothelial cell (LuEC) population. We defined our population as a CD45 negative, CD31 and CD102 positive population[45, 46]. The antibodies used for our experiments are listed in Table 4.

Murine lung single cells in FACS Buffer were equally distributed to 6 FACS tubes per sample to obtain single stained, fully stained and unstained sample for each probe and centrifuged at 1250 rpm for 5 min. The supernatant was discarded, cells were resuspended in FACS buffer containing antibodies at concentrations of 1-2µg/ml and incubated in dark on ice for 30min. After two washing and centrifugation steps, the cells were resuspended in 300µl FACS buffer and analyzed on a LSRII Fortessa flow cytometer using FACS DIVA Software (BD Biosciences, Franklin Lakes NJ, USA). Gates were set for exclusion of cell fragments, doublets, dead cells and CD45 positive cells. The CD45

negative cells were divided by CD31/CD102 positivity and the double positive population was defined as the lung endothelial cell population of interest[45, 46] (figure 3). Compensation with single stainings were performed and at least 100 000 events were recorded. Final data analysis was performed with FlowJo 10.4.1 software (FlowJo, LLC, Ashland OR, USA).

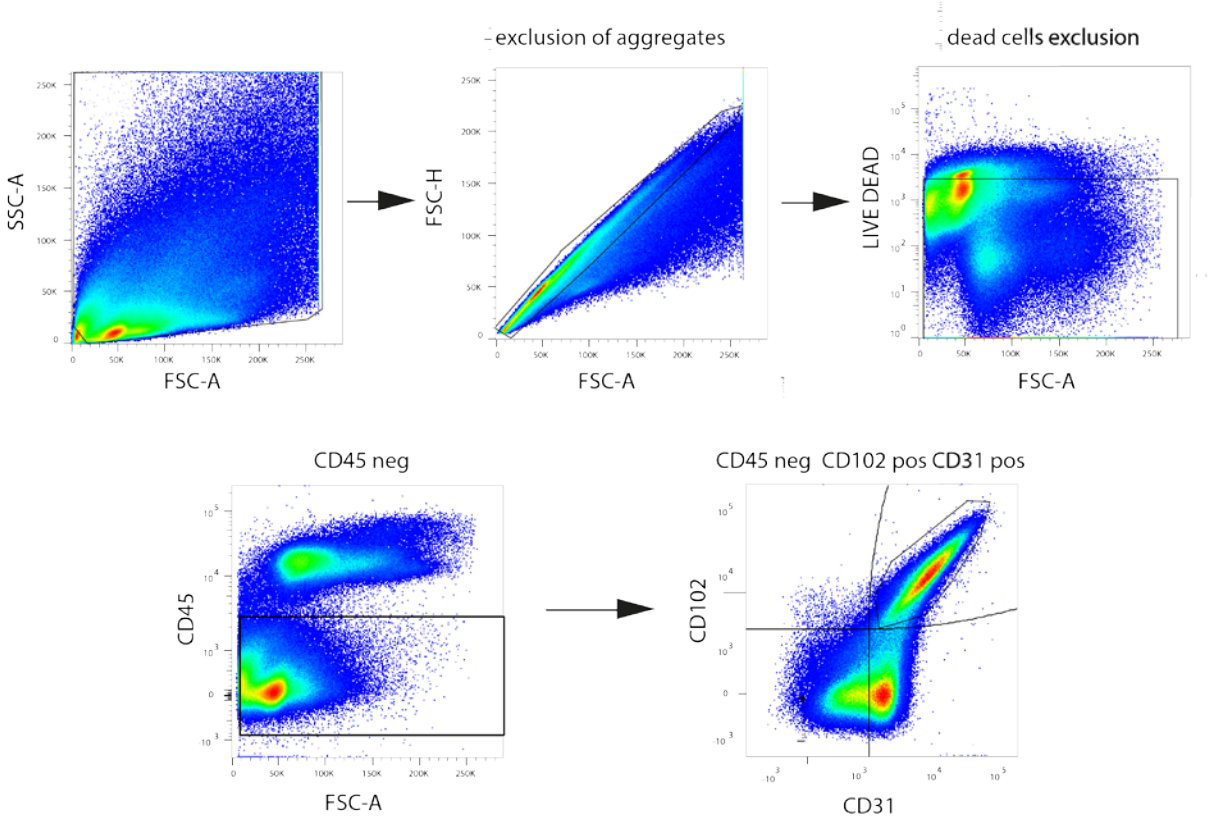

Figure 3: Gating strategy of heme ±LPS in vivo treated murine lung endothelial cells (LuEC)
All in vivo samples for FACS Sorting were labelled with following fluorescent antibodies: LIVE-DEAD IR, CD45 (=Protein tyrosine phosphatase, receptor type, C)-, CD31(=PECAM-1)- and CD102(=ICAM-2)- antibody. CD45 negative, CD31 and CD102 positive populations were used for further analysis.

Table 4: Antibodies used for flow cytometry

Gene	**Order Number**		
Antibody	**Cluster of differentiation**	**Label**	**Company**
LIVE/DEAD		Near IR (APC-Cy7)	Invitrogen
anti-mouse CD45.2	CD45/ PTPRC	Pacific Blue	Bio Legend
rat-anti-mouse CD102	CD102/ICAM2	FITC	BD Biosciences
rat-anti-mouse CD31	CD31/PECAM1	APC	BD Biosciences

4.12.2 Fluorescent Activated Cell Sorting

Fluorescent Activated Cell Sorting (FACS Sorting) was applied to obtain lung endothelial cells for further analysis by RT-qPCR. Murine lung single cell suspension was prepared and stained as described above for FACS and sorted on the BD FACSAria™ III instrument (BD Biosciences) with gate settings implemented for the flow cytometry analysis. 70'000 CD45 negative, CD31/CD102 positive cells were sorted in a 1.5ml microtube containing 150µl RLT Lysis Buffer (QIAgen). 1% 2-Mercaptoethanol was added directly after the sorting and the cell lysate was kept at -80°C for RNA Isolation.

4.12.3 RNA Isolation and RT-qPCR from murine lung endothelial cells

RNA from FACS sorted lung endothelial cells was isolated using RNeasy® Micro Kit (QIAgen) according to the manufacturer's protocol. 7.7µl of purified RNA were reverse transcribed to cDNA with TaqMan Reverse Transcription reagents (Applied Biosystems, Carlsbad CA, USA) as described above. cDNA was spectrophotometrically quantified and checked for quality and then diluted with DNAse free water to approximate 300 ng/µl. FAM qPCR with TaqMan FAST Universal PCR Mastermix was performed using 2µl of diluted cDNA. Change of VCAM-1 expression was normalized to unregulated reference gene HPRT and displayed as $log2^{-\Delta CT}$. FAM-labeled primers used in this experiment are listed in Table 3.

4.13 In vivo experiment for heme ± anti-CD40 in mice

We used an in vivo model of agonistic anti-CD40 induced murine necroinflammatory liver disease as a TLR4-independent NFκB agonist [24]. Wild-type C57BL/6J animals were obtained from Charles River (Wilmington, MA, USA) and further bred in the LASC animal facility under standard conditions as described above. The animals were divided into 4 treatment groups and received treatment with either heme-albumin (protocol described in heme-albumin preparation) or anti-CD40 (anti-mouse CD40; BioXCell, West Lebanon, USA) as follows: Control animals remained untreated; the heme-

albumin group was treated with singular i.p. injections of heme-albumin (70µM/kg body weight). The third group was pretreated with heme-albumin i.p. (70µM/kg body weight) for 4h and then received i.p. injections of anti-CD40 (10mg/kg body weight). The fourth group received the same dose of anti-CD40 i.p at the same time point as the previous group. The animals were sacrificed 24h after anti-CD40 injection for blood collection, or 48h after anti-CD40 administration for liver collection. The experimental protocol was approved by Veterinary Office of the Canton of Zurich under the license number 014/2017.

4.13.1 Liver collection for histology and H&E staining

Liver lobes from mice were removed, rinsed in PBS and placed in 10% formalin solution (Sigma-Aldrich, St.Louis, USA) for fixation. The organs were transferred to 70% ethanol after 48h. Paraffin embedding and microtome sectioning (3µm) were done by the Institute of Veterinary Pathology, Vetsuisse faculty, University of Zurich. The slides were stained with H&E staining using hematoxylin (hematoxylin solution, Harris modified, Sigma-Aldrich) and eosin solution (eosin y solution, aqueous, Sigma-Aldrich) according to standard manufacturer's protocol. Histology images were obtained using Zeiss AxioObserver Z1 microscope with AxioCam MRm and 10x objective and scanned with ZEN software (all Carl Zeiss AG, Feldbach, Switzerland).

4.13.2 Blood collection and liver enzyme measurement

Terminal blood collection through heart punction of anesthetized mice was performed and blood was immediately transferred to heparin coated 0.5ml tubes. To obtain plasma, the heparin tubes were centrifuged for 10min at 3000xg at 4°C. The plasma was transferred to 1.5ml Eppendorf tubes and 32µl were used immediately for liver enzyme measurement using a Reflotron Plus clinical chemistry system (Roche Diagnostics, Basel, Switzerland). Levels of alanine transaminase (ALT) and aspartate transaminase (AST) were determined in each sample.

4.14 Statistics

Data were analyzed with Graph Pad Prism 7 software (Graph Pad software, San Diego, CA). T-test to compare two variables or one-way ANOVA with Tukey's multiple comparison test for more than two variables were used for statistical analysis. The significance threshold was set to $p < 0.05$.

5 Results

5.1.1 Heme-albumin suppresses IL-1β-induced upregulation of adhesion molecules on endothelial cells in vitro

RT-qPCR

Quantitative RT-PCR was used to demonstrate the changes in mRNA levels of pro-inflammatory adhesion molecules VCAM-1 and E-selectin. We could show a significant suppression of VCAM-1 and E-Selectin levels in the heme-albumin+IL-1β (100U/ml) treated HUVEC compared to cells treated with IL-1β (100U/ml) alone. The degree of heme-mediated suppression of mRNA expression of VCAM-1 and E-selectin was dose-dependent (Fig. 4). There were no significant changes between the mRNA levels of VCAM-1 and E-selectin in untreated samples (ctrl) and the samples treated with heme-albumin 80 and 160µM.

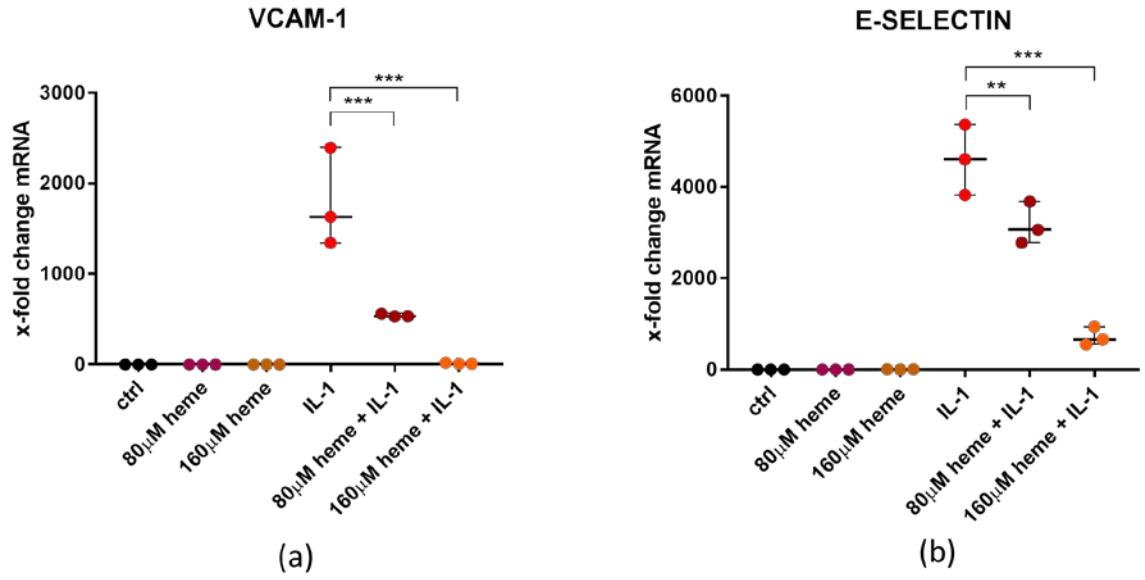

Figure 4: heme-albumin suppresses upregulation of IL-1β-induced VCAM-1 and E-selectin mRNA expression
Real-time PCR quantification of relative mRNA expression of proinflammatory adhesion molecules on HUVEC in response to heme-albumin 80 or 160µM ± human IL-1β 100U/ml vs. IL-1β 100U/ml stimulation. Ctrl=untreated cells. Data are shown in triplicates (n=3). Statistical significance (one-way ANOVA with Tukey's multiple comparison test) is displayed as follows: ***=p<0.001, **=p<0.01

VCAM-1 In-Cell Western Immunofluorescent Assay

With the In-cell Western Immunofluorescent Assay, we were able to confirm the results of the previous RT-qPCR analysis on protein levels of formaldehyde fixed cells. Namely, we could demonstrate the suppression of VCAM-1 protein expression on IL-1 stimulated HUVEC in presence of heme-albumin. In the image taken with the infrared imager (LI-COR) (see Fig.5a), we can clearly recognize the green signal correlating with IL-1 (100U/ml) mediated VCAM-1 expression. We observe a complete suppression of IL-1 response by heme in a dose-dependent manner. Figure 5b shows the 800nm/700nm quotient of relative fluorescent units from the same experiment. No signal for VCAM-1 expression was observed on cells treated with heme-albumin alone (Fig.5a and b).

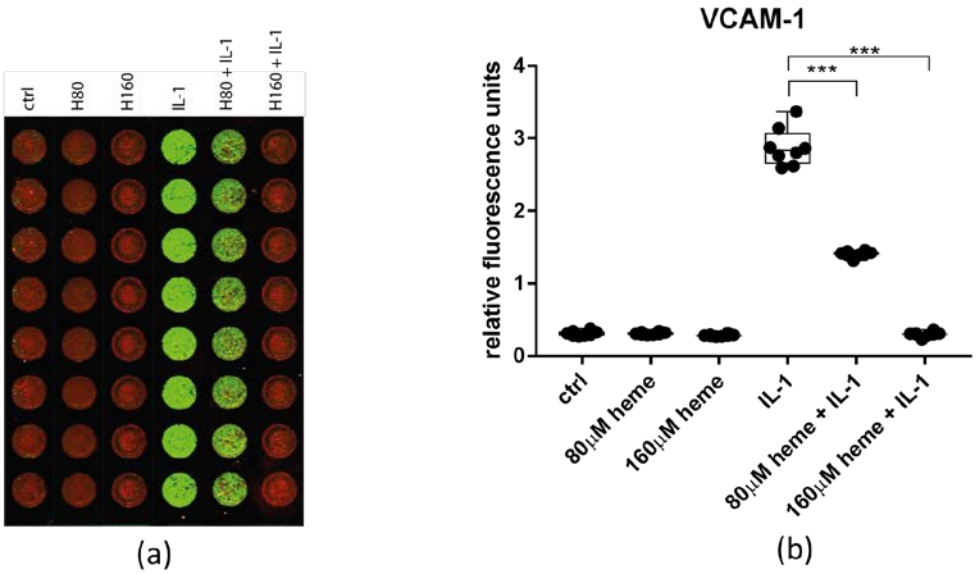

Figure 5: heme-albumin suppresses IL-1β induced VCAM-1 expression on HUVEC cell surface
(a): In-cell Western Immunofluorescent Assay image showing VCAM-1 signal (green) and live-cell DNA stain DRAQ5 (red) in response to heme-albumin 80 or 160μM (H80, H160) ± human IL-1β 100U/ml (IL-1) or IL-1β 100U/ml stimulation. Ctrl=untreated cells. (b) Quantification of VCAM-1 signal expressed relative to live-cell DNA stain DRAQ5 in relative fluorescence units of the same experiment as in (a). Data are shown in octuplicates (n=8). Statistical significance (one-way ANOVA with Tukey's multiple comparison test) is displayed as follows: ***=p<0.001

5.1.2 Heme-albumin suppresses IL-1β-induced inflammatory chemokine release from endothelial cells in vitro

IL-8 Immunoassay

To investigate the effect of heme-albumin on chemokine release under inflammatory conditions, we measured IL-8 concentrations in HUVEC culture supernatants. IL-8 secretion of IL-1β stimulated HUVEC is significantly ($p<0.001$) suppressed upon 4h pretreatment with heme-albumin (Fig.6). These results show again a dose-dependent effect. Moreover, no IL-8 secretion was observed in cells treated with heme-albumin alone.

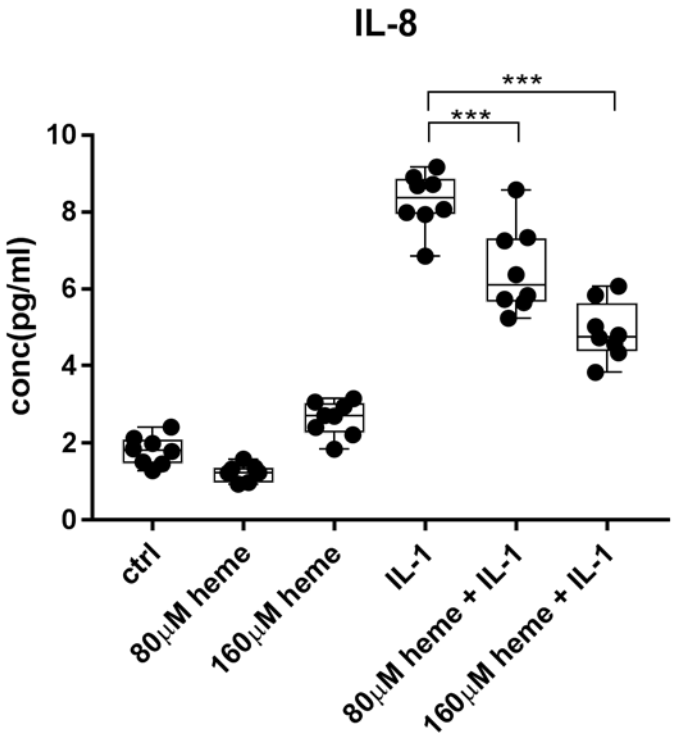

Figure 6: heme-albumin suppresses IL-1β-induced inflammatory chemokine IL-8 release from HUVECs

IL-8 concentrations (conc) in pg/ml measured in Bio-Plex Immunoassay in response to heme-albumin (heme) 80 or 160μM ± human IL-1β 100U/ml (IL-1) or IL-1β 100U/ml stimulation in HUVEC supernatants. Ctrl=untreated cells. Data are shown in octuplicates (n=8). Statistical significance (one-way ANOVA with Tukey's multiple comparison test) is displayed as follows: ***=$p<0.001$

Monocyte Adhesion Assay

Next, we investigated adherence of LPS-activated monocytes to endothelial cells to confirm the functional relevance of heme-albumin triggered suppression of IL-8 release and VCAM-1 expression upon IL-1β stimulation. Adherence of activated monocytes was maximal to IL-1β stimulated HUVEC. Heme-albumin pretreatment causes significant ($p<0.001$) dose-dependent decrease in monocyte adherence to IL-1β activated HUVEC (see Fig.7). HUVEC cells pretreated with heme-albumin in doses of 80-160μM showed minimal monocyte adhesion.

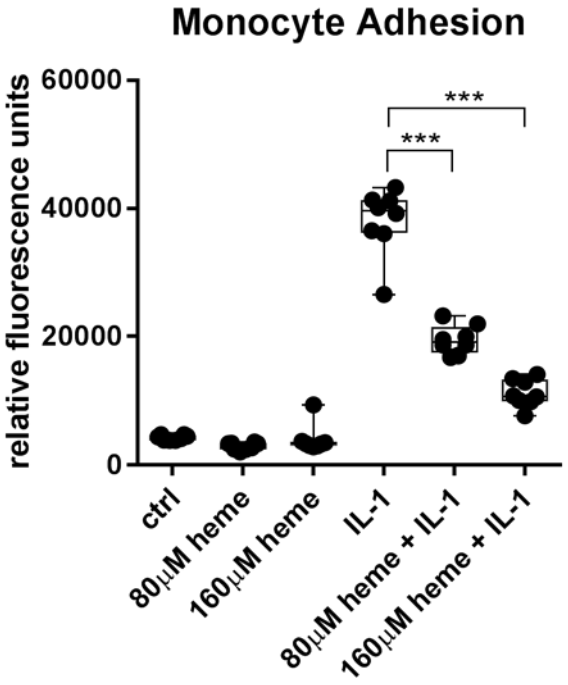

Figure 7: heme-albumin suppresses IL-1β-induced activated monocyte adhesion on HUVEC

Quantification of LPS-activated and fluorescence-labeled monocyte adhesion to HUVEC, which were pretreated with heme-albumin (heme) 80 or 160μM ± human IL-1β 100U/ml (IL-1) or IL-1β 100U/ml stimulation. Ctrl=untreated HUVEC. Data display fluorescence units' measurement at 520nm of treatment in octuplicates (n=8). Statistical significance (one-way ANOVA with Tukey's multiple comparison test) is displayed as follows: ***=$p<0.001$

5.1.3 Heme-albumin effect on endothelial barrier function

Electric Cell-substrate Impedance Sensing (ECIS)

The endothelial barrier function of confluent monolayers of HUVEC were studied before and during the treatment with increasing concentrations of heme-albumin. Impedance measurement of all 15 wells started 8h before treatment. At confluency, when impedance reached a plateau, time point 0 was set and the impedance was normalized to 1. The cells were stimulated at time point 0 with 0, 40, 80 or 160µM heme-albumin in triplicates. Impedance was continuously recorded for further 12h (Fig. 8). The first drop in the normalized impedance in all wells, as seen in Figure 8, at time point 0 is an artefact caused by manipulating the well during application of stimuli. 2h after stimulation, the impedance levels were balanced back to a constant value. The impedance of untreated and heme-albumin 40 and 80µM treated cells does not vary significantly over the time recorded (Fig.8). The impedance values of the heme-albumin 160µM stimulated cells drop during the first 6h of treatment by approximately 50%. Thereafter, the impedance starts to rise again 8h after stimulation. The cell impedance of heme-albumin 320uM treated cells decreases already at 2h and remains at very low level for the rest of the recorded time (Fig. 8).

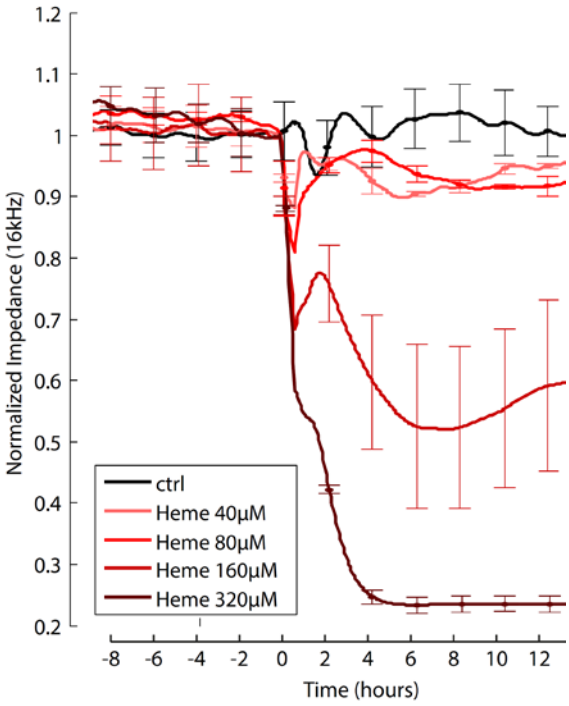

Figure 8: heme-albumin effect on endothelial barrier function

HUVEC were grown to confluent monolayers on ECIS 8well chamber slides. Electric cell impedance at 16kHz over time was measured in triplicates per treatment using ECIS® technology. Impedance was normalized to 1 at timepoint 0. HUVECs were stimulated with 0 (ctrl), 40, 80, 160 or 320µM heme-albumin (heme) at timepoint 0. Data represent means ± SD from 8h before to 12h after stimulation

5.1.4 Heme-albumin-induced hypoinflammation in endothelial cells is not caused by the impairment of metabolic function

Extracellular Flux Assay

To exclude that the above described heme-mediated hypoinflammatory effect on adhesion molecule expression, chemokine release and the changes in barrier function shown in ECIS experiment are all caused by heme toxicity, we measured mitochondrial function and glycolytic rate in heme-albumin treated cells with a XF Cell Mito stress test using a Seahorse extracellular flux analyzer, as described in Methods.

There was no impairment of metabolic function of HUVEC pretreated with heme-albumin 80 or 160µM for 6h (Fig. 9). The oxygen consumption rate profile (OCR) (Fig. 9a) is similar in untreated HUVEC and cells treated with heme-albumin 80µM and heme-albumin 160µM, respectively. Likewise, the extracellular acidification rate (ECAR), which measures the proton (H^+) production in glycolysis after addition of different mitochondrial inhibitors, was constant in the both untreated and heme-albumin treated HUVEC (Fig. 9b), excluding heme-mediated toxicity at concentrations where a suppressive effect on inflammation was observed. One representative experiment from the experimental series of 3 is shown in Fig. 9.

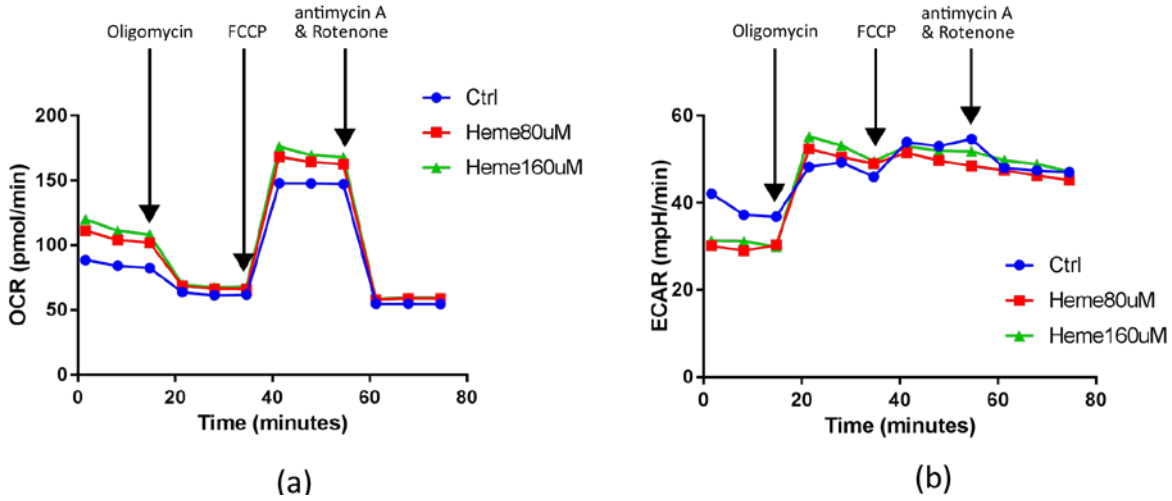

Figure 9: heme-albumin effect on metabolic functions of HUVEC

(a): Extracellular flux analysis of oxygen consumption rate (OCR, pmol/min) of HUVEC treated with 0, 80 and 160 µM heme-albumin (heme) for 6h.
(b): Extracellular acidification rate (ECAR, mpH/min) of HUVEC treated with 0, 80 and 160µM heme-albumin (heme) over 6h. Every line corresponds to one well with 40'000 cells

5.1.5 Heme-albumin suppresses LPS-induced inflammatory response in murine lung endothelial cells in vivo

RT-qPCR

VCAM-1 mRNA expression was measured by RT-qPCR as read-out for activation of pro-inflammatory NFκB pathway in endothelial cells in an LPS-induced inflammation mouse model in vivo. As described above, LPS causes activation of leucocytes, especially monocytes. They release their typical pro-inflammatory cytokines IL-1β and TNFα and thus activate endothelial cell inflammatory response. We isolated RNA from lung endothelial cells from B6 mice treated with heme-albumin 100µmol/kg body weight ± LPS 0.5mg/kg body weight and then performed a RT-qPCR. As shown in Fig.10, VCAM-1 mRNA expression on lung endothelial cells of LPS-challenged animals was significantly suppressed when mice were pretreated with heme-albumin.

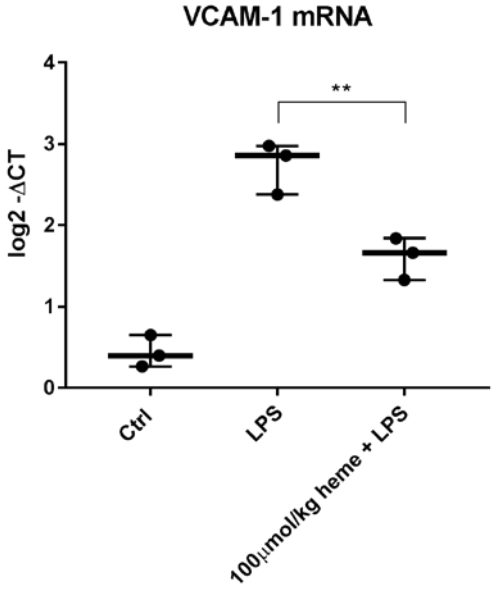

Figure 10: heme-albumin suppresses upregulation of LPS induced VCAM-1 mRNA expression on lung endothelial cells in wild-type animals in vivo

Real-time PCR quantification of mRNA expression given as $log2^{-\Delta CT}$ of VCAM-1 on murine LuEC in response to 4h LPS 0.5mg/kg body weight ± overnight heme-albumin 100µmol/kg body weight pretreatment. Ctrl=untreated animals. Data represent triplicates (n=3). Statistical significance (one-way ANOVA with Tukey's multiple comparison test) is displayed as follows: **=p<0.01

5.1.6 Heme-albumin rescues anti-CD40-induced necroinflammatory liver disease in mouse

Macroscopic and histological analysis

To explore the immunomodulatory effect of heme-albumin in anti-CD40 induced necroinflammatory liver disease we collected liver lobes from heme-albumin ± anti-CD40 treated B6 mice. We observed that treatment of animals with agonistic anti-CD40 leads to ischemic liver infarctions, which coincide with histological evidence of arterial thrombosis seen in Fig. 12c. In the macroscopic image of the liver lobe from an anti-CD40-treated mouse, we see white areas corresponding to necrotic zones (Fig.11 b). The macroscopic image of the liver lobe from heme-albumin + anti-CD40 treated animal, the white areas are not present (Fig. 11 c). In the corresponding histological analysis we can clearly recognize areas of ischemic tissue necrosis with perivascular immune cell infiltrations in the anti-CD40 liver image (Fig. 13 c). Moreover, we identified the necrotic zones mostly in perivascular regions around numerous thromboses, as seen in detail in Fig.13c (*) and in the overview image in Fig.12c(*). Figure 12d and 13d show the typical histologies of the liver lobes from heme-albumin and anti-CD40 treated animals, where ischemic necrotic areas are missing. The histology of the liver lobes from control and heme-albumin treated animals does not show any tissue injury (Fig.12a,b and Fig.13a,b).

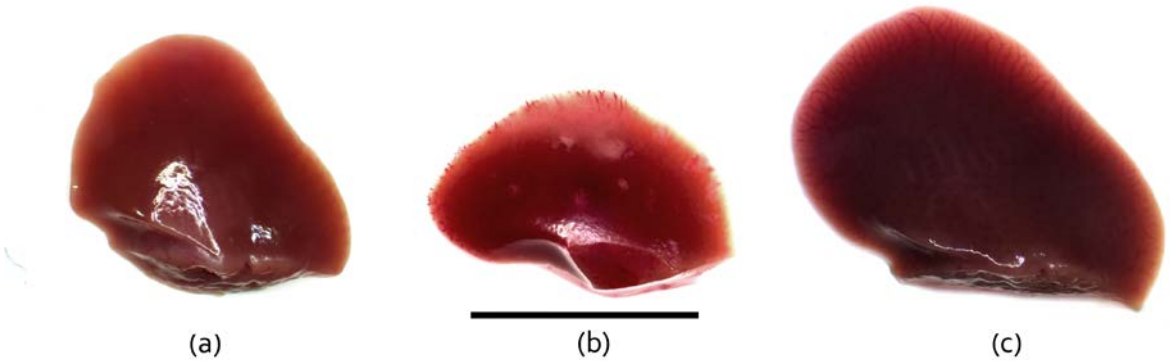

Figure 11: heme-albumin rescues anti-CD-40 induced liver necrosis

(a) Control **(b)** anti-CD40 10mg/kg body weight **(c)** heme-albumin 70µM/kg body weight+ anti-CD40 10mg/kg body weight

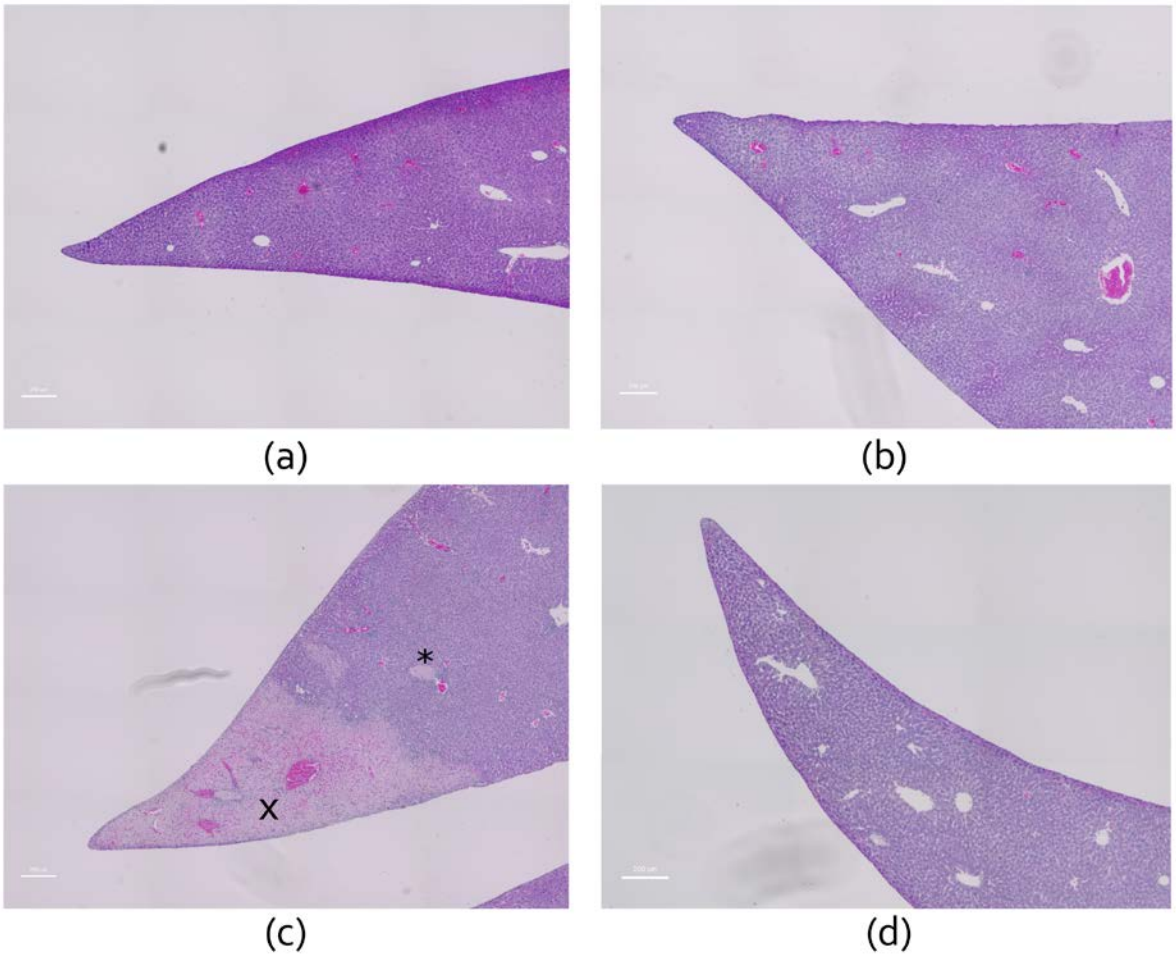

Figure 12: heme-albumin rescues anti-CD40-induced liver necrosis

(a) Control **(b)** heme-albumin 70µM/kg body weight

(c) anti-CD40 10mg/kg body weight **(d)** heme-albumin 70µM/kg body weight+ anti-CD40 10mg/kg body weight. thrombosis (*), necrosis (x); original magnification, x10.

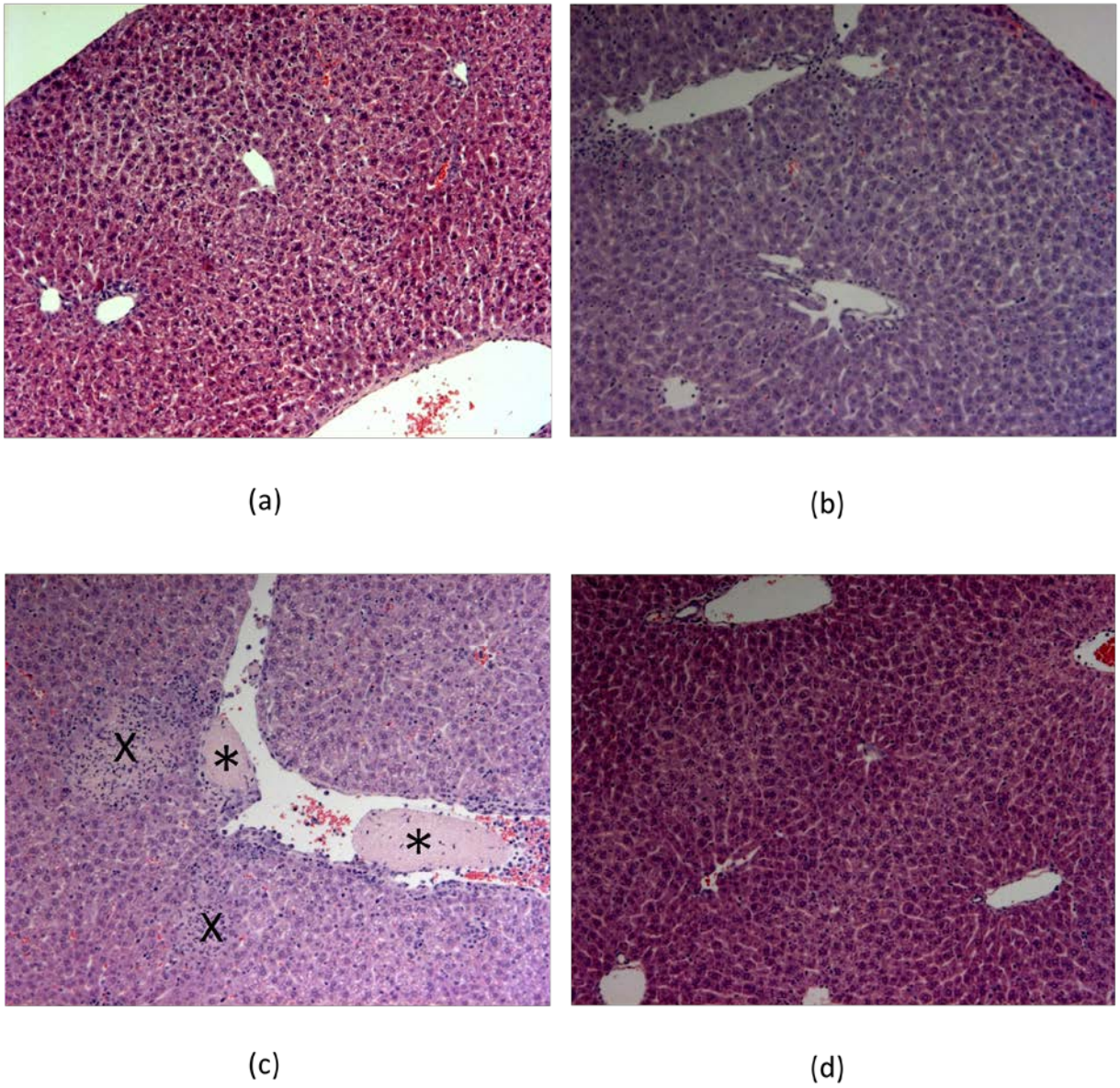

Figure 13: heme-albumin rescues anti-CD40-induced liver necrosis

(a) Control **(b)** heme-albumin 70µM/kg body weight
(c) anti-CD40 10mg/kg body weight **(d)** heme-albumin 70µM/kg body weight+ anti-CD40 10mg/kg body weight. **(*)** thrombosis, **(x)** necrosis and immune cell infitrates; original magnification, x10

Liver enzymes

To quantify the extent of ischemic infarctions, we measured levels of the liver enzymes alanine transaminase (ALT) and aspartate transaminase (AST) in plasma of mice. As shown in figure 14, levels of liver enzymes ALT and AST 24h after anti-CD40 administration are significantly elevated compared to untreated animals. The elevation of ALT and AST was significantly reduced in the heme-albumin pretreated (heme+ anti-CD40) group (p=0.013 for ALT and p=0.03 for AST) compared to anti-CD40 treated animals. Moreover, the levels of ALT and AST in untreated and heme+ anti-CD40 treated animals showed no significant difference.

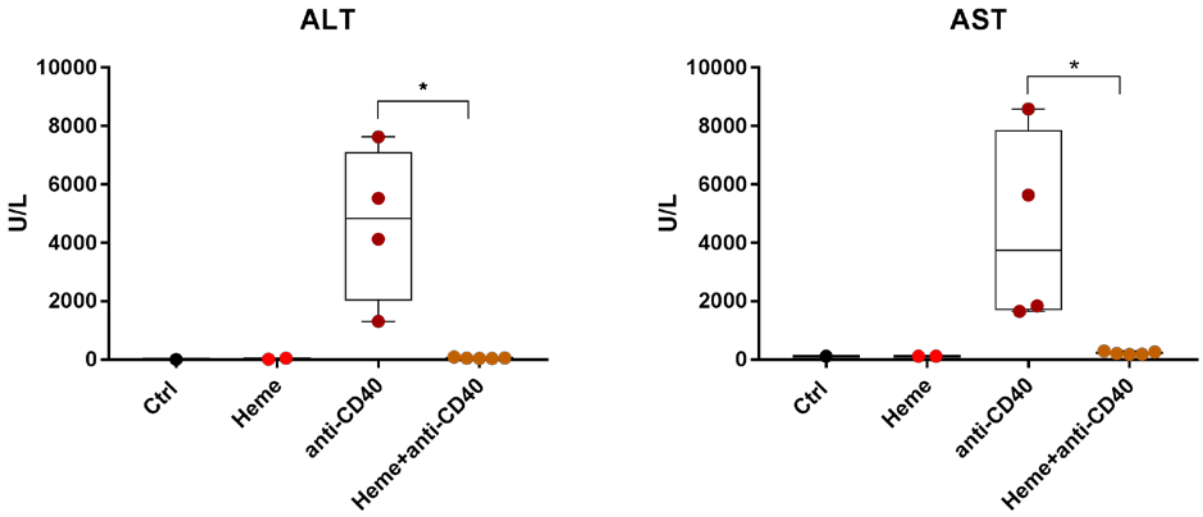

Figure 14: levels of ALT and AST show rescue of anti-CD40-induced liver necrosis after heme-albumin
Alanine transaminase (ALT) and aspartate transaminase (AST) plasma levels of wild-type (B6) mice treated with heme-albumin 70µM/kg body weight, heme-albumin 70µM/kg body weight + anti-CD40 10mg/kg body weight or anti-CD40 10mg/kg body weight alone. Ctrl=untreated animal. Data represent biological replicates, whereat every dot on the graph represents one animal. Statistical significance (one-way ANOVA with Tukey's multiple comparison test) is displayed as follows:
* =p<0.05

5.2 Heme-albumin-mediated hypoinflammation in endothelial cells is Hmox-1-independent and related to Nrf2 activation

Because of its close association to heme and its anti-inflammatory properties, a significant role of Hmox-1 in heme-dependent hypoinflammation must be assumed. To study Hmox-1 effect, we used inducible Hmox-1 knock-out (UBC cre-ERT2 +/- Hmox-1 flox/flox) mouse model to look at the heme effect on endothelial inflammatory response in Hmox-1 free system. Using gene array analysis, we aimed to dissect the underlying gene expression pattern behind the effects of heme-albumin on HUVEC (data not shown). Heme treatment was characterized by upregulation of the following genes; hemoxygenase 1 (Hmox-1), NAD(P)H dehydrogenase [quinone] 1 (NQO1), sodium-independent cystine-glutamate antiporter (Scl7a11) and glutathione-disulfide reductase (GSR), which were identified as Nrf2 target genes [47, 48]. Therefore, we decided to look closer at the role of the enzyme Hmox-1 and the transcription factor Nrf2 in the heme-mediated hypoinflammation in endothelial cells.

5.2.1 Heme-albumin-mediated hypoinflammation is Hmox-1 independent

RT-qPCR

To investigate a predominant effect of Hmox-1 in the heme-induced suppression of the NFκB-dependent inflammatory response in vivo, we used UBC cre-ERT2 +/- Hmox-1 flox/flox mice, treated them with tamoxifen as described in the method section, and obtained Hmox-1 knock-out animals. Thereafter, the mice were treated with heme-albumin 50µmol/kg body weight overnight and challenged with LPS 0.5mg/kg body weight for 4h each. As seen in Fig. 15, the LPS induced overexpression of VCAM-1 mRNA in murine hmox-ko LuEC is significantly suppressed by heme-albumin pretreatment.

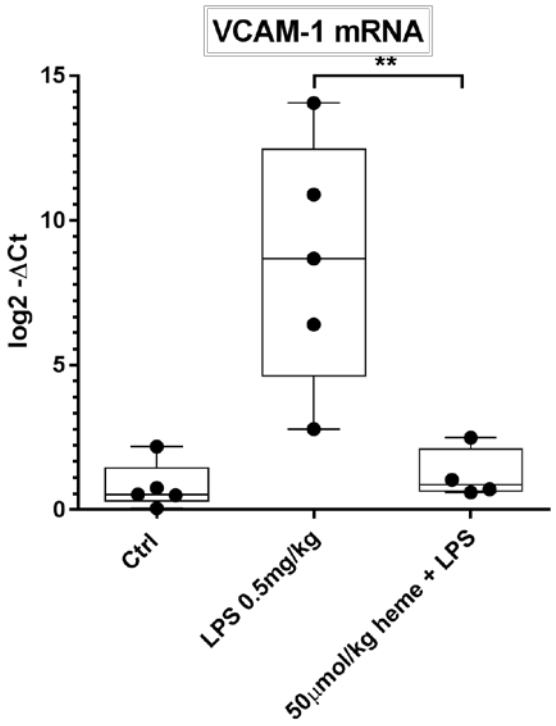

Figure 15: heme-albumin suppresses upregulation of LPS-induced VCAM-1 mRNA expression on lung endothelial cells in hmox-1 knock-out animals in vivo

Real-time PCR quantification of VCAM-1 mRNA expression, given as $log2^{-\Delta CT}$ in murine LuEC in response to 4h LPS 0.5mg/kg body weight ± overnight heme-albumin 50µmol/kg body weight pretreatment. Ctrl=untreated animals. Every data point represents 1 mouse. Data represent replicates from 3 experiments. Statistical significance (one-way ANOVA with Tukey's multiple comparison test) is displayed as follows: **=p<0.01

5.2.2 Heme-albumin causes Nrf2 activation in vitro

RT-qPCR

We performed a RT-qPCR experiment and looked at changes in mRNA expression of the Nrf2 target genes NQO1, Slc7a11, GSR and Hmox-1. Our results revealed significant upregulation of all Nrf2-dependent target genes after heme-albumin treatment compared to untreated controls. Moreover, the induction was heme dose-dependent (Fig.16). In detail, NQO1 mRNA expression was 5-fold higher in heme 80µM treated ($p<0.01$), and approx. 7-fold higher in 160µM treated ($p<0.001$) compared to untreated HUVEC. Scl7a11 mRNA expression was approx. 6-fold (80µM; $p<0.05$) and 9-fold (160µM; $p<0.01$) elevated with heme-albumin compared to untreated HUVEC. GSR mRNA levels increased approx. 2-fold (80µM; $p<0.05$) and 6-fold (160µM; $p<0.001$) in heme-albumin treated compared to untreated HUVEC. Hmox-1 mRNA expression was approx. 70-fold (80µM, not significant), and 800-fold (160µM; $p<0.05$) upregulated in heme-albumin treated cells compared to controls. For Hmox-1, (in Fig. 16) 1500-fold change in mRNA expression in one of the 160µM heme-albumin samples stands clearly out. 20µM RA839 (Nrf2 activator) treated HUVEC were add to the experimental system as positive controls for Nrf2 induction.

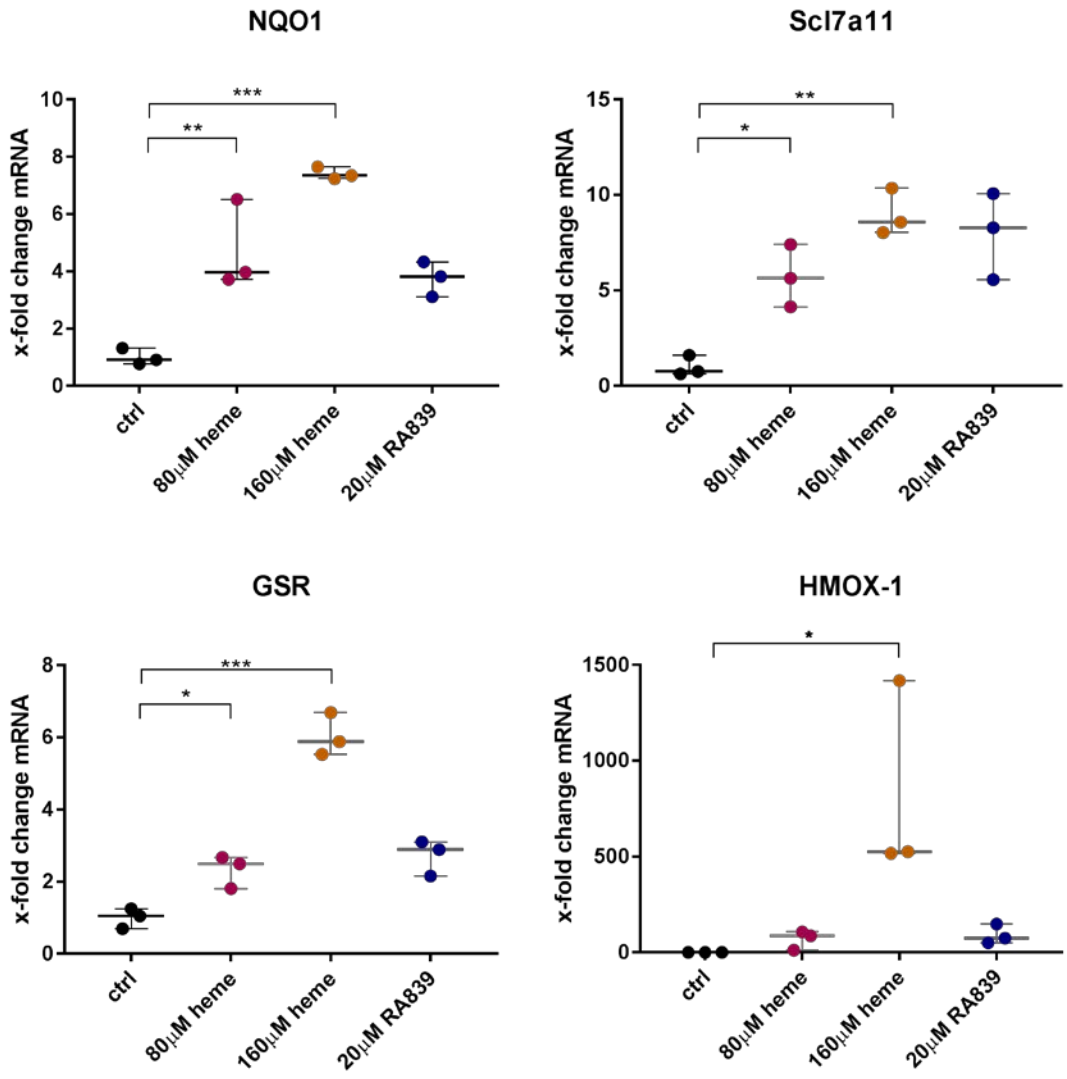

Figure 16: heme-albumin causes Nrf2-activation and upregulation of Nrf2-dependent genes in vitro

RT-qPCR quantification of relative mRNA expression of Nrf2-dependent genes NQO1, Scl7a11, GSR and Hmox-1 in HUVEC in response to heme-albumin 80 or 160μM or Nrf-2 activator RA839 20μM. Ctrl=untreated cells. Data represent triplicates (n=3). Statistical significance (one-way ANOVA with Tukey's multiple comparison test) is displayed as follows: ***=p<0.001, **=p<0.01, * =p<0.05

Nrf2 Translocation Assay

To explore the Nrf2 activation and its translocation in nucleus, we collected cytoplasmic and nuclear fractions of proteins and looked for presence of Nrf2 in the nuclear fraction. As shown in figure 17, Nrf2 concentration in nucleic fraction of HUVEC protein lysate is higher in heme-albumin 80µM treated cells compared to untreated cells and it is comparable to the Nrf2 concentration in the Nrf2 activator RA 839 treated cells.

Hence, heme-albumin enhances nuclear translocation of Nrf2 in HUVEC after 6h of treatment. β-Actin was used as a loading control on the same membrane as shown in Fig. 17, lower line.

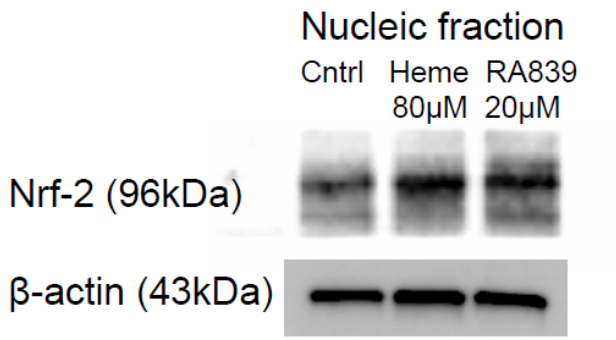

Figure 17: heme-albumin causes Nrf2 translocation in nucleus

Representative Western blot of nuclear Nrf2 levels in Control, Heme 80µM and Nrf-2 activator RA 839 20 µM treated HUVEC after 6h of treatment (upper line). β-Actin was used as loading control (lower line)

5.2.3 Heme-albumin causes Nrf2 activation and upregulation of Nrf2 target genes in vivo

RT-qPCR

To look at Nrf2 activation in vivo, we analyzed samples from our in vivo heme+LPS experiment in wild-type mice (same samples as in Fig. 10) for mRNA expression of the Nrf2 target genes Hmox-1 and Slc7a11. As shown in Figure 18, we can observe a tendency towards increased Hmox-1 and Slc7a11 mRNA expression in heme-albumin pretreated sample.

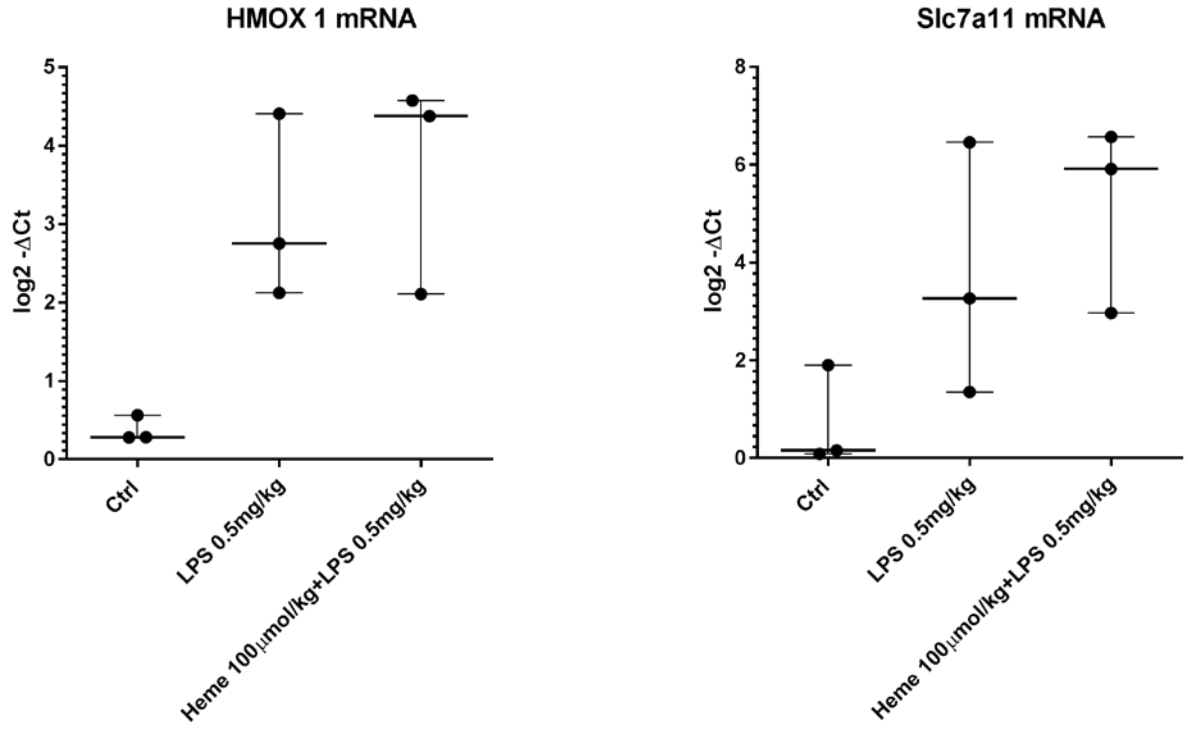

Figure 18: heme-albumin modulation of Nrf2 target gene expression in vivo

Real-time PCR quantification of mRNA expression given as $log2^{-\Delta CT}$ of Nrf2 target genes Hmox-1 and Scl7a11 in wild type mice in response to overnight heme-albumin 100µmol/kg body weight ± 4h LPS 0.5mg/kg body weight or 4h LPS 0.5mg/kg body weight i.p. treatment. Control=untreated animals. Every data point represents 1 mouse. Data represent replicates from 3 experiments

6 Discussion

Until today, the exact role of heme in hemolytic conditions like sickle cell disease, malaria or sepsis is not fully understood. Endothelial cells as sentinels for intravascular pathological processes are major initiators of immune system responses [14, 18]. Their interaction with free hemoglobin and heme and their role in the initiation of inflammatory responses is a key element for understanding why intravascular hemolysis causes severe clinical condition.

6.1 Heme suppresses inflammatory responses in endothelial cells

Our data indicate a suppressive role of heme on endothelial inflammation. We demonstrated suppressive effects of heme-albumin on IL-1β-induced mRNA overexpression of the adhesion molecules VCAM-1 and E-selectin in HUVEC in vitro (Fig.4 and 5). Furthermore, we presented heme-albumin driven suppressive effects on chemokine production by looking at IL-8 release from activated endothelial cells (Fig. 6). Consistent with these data, we observed a significant decrease of monocyte adhesion on IL-1 β stimulated HUVEC (Fig. 7).

By real-time assessment of the barrier function of HUVEC monolayers during stimulation with increasing doses of heme-albumin, we could show that endothelial barrier function remains stable upon treatment with 40-80µM heme-albumin, deteriorates transiently upon treatment with 160µM heme-albumin and permanently upon treatment with 320µM heme-albumin, respectively (Fig. 8).

To exclude heme-dependent cellular toxicity as a possible reason for heme-induced suppression of inflammatory responses and for changes in endothelial barrier function, we demonstrated that the mitochondrial function is not impaired by heme-albumin treatment in vitro, especially in cells treated with 160µM heme-albumin (Fig. 9).

We suggest that previous reports of pro-inflammatory effects of heme might have been influenced by the difficult biophysical properties of purified (protein-free) heme [49]. For the hydrophobic molecule heme, it is very unlikely to occur in considerable quantities in free, monomeric form in

plasma because of its tendency to bind to different hemoproteins like hemoglobin and myoglobin, or to albumin [5]. Many in vitro experiments suggesting a pro-inflammatory role of heme were carried out under serum-free conditions [50-52], where the amount of free, non-protein bound heme is much higher than in the serum-enriched medium. Different experiments with heme mixtures were previously conducted in our laboratory and the amount of free heme in our heme-albumin mixture was usually around 10% compared to the standard heme-NaOH mixture, which contained around 80% of free heme (data not shown). Therefore, we postulate that heme bound to a carrier protein albumin, instead of free heme, corresponds better to the physiological state in living organism.

Heme drives anti-inflammation in lung endothelial cells in LPS-induced inflammatory mouse model

To examine the effect of heme on the endothelial cell immune response in vivo, we used 2 inflammatory mouse models. First, we demonstrated that heme-albumin suppresses the inflammatory response in LPS-induced inflammatory mouse model by showing heme-mediated suppression of VCAM-1 expression on murine lung endothelial cells in vivo (Fig. 10). The activation of the endothelial inflammatory response might be caused directly by activation of TLR4 by LPS on the endothelial cell surface or indirectly by LPS-induced activation of innate immune cells like monocytes and their production of pro-inflammatory cytokines IL-1β and TNFα, which activate endothelial cells [14, 17].

Heme-mediated rescue effect in an anti-CD40 induced ischemic liver necrosis mouse model

A model of necroinflammatory liver disease caused by administration of an agonistic monoclonal antibody anti-CD40 in mice was reported, and a pivotal role of B-cell and macrophage induced TNFα and INFγ in this model was described [24]. However, the exact mechanism of necrosis development and the role of vascular endothelial cells in this model remained ambiguous.

Here we report a novel observation that heme provides rescue from anti-CD40 induced necroinflammatory liver disease. As shown in Fig. 11b and 12c, single administration of anti-CD40 to mice causes development of extensive necrotic areas throughout the liver tissue. Remarkably, we identified the necrosis areas mostly in perivascular regions and discovered numerous thromboses in the vessels surrounded by necrotic zones (Fig 12c and 13c). Heme challenge suppresses the phenotype of the disease as suggested by the absence of necrotic lesions (Fig. 11c, 12-13d) and the pronounced decrease of transaminase levels (Fig. 14).

The limitation of these in vivo data is the overall small number of animals and the uneven number of data points per each treatment group. This fact was due to limited number of available animals and due to technical limitations of our blood collection method. These data represent single experiment from our experimental series and can therefore support our hypothesis, but not definitely prove the heme rescue effect on anti-CD40 induced liver necrosis. Further experiments are already ongoing and may provide additional evidence for our hypothesis in the near future.

In summary, the anti-CD40 related findings support our previous results that heme has an anti-inflammatory effect, and show that heme can prevent anti-CD40 dependent necroinflammatory liver injury. Nonetheless, several questions remain open and need to be discussed.

First, the role of endothelial cells and their interaction with the immune cells in the described anti-CD40 induced necroinflammatory desease has to be proven by future research. The observation of thrombosis in the liver vasculature after anti-CD40 administration provides a strong sign that

endothelial cell activation may be involved in the pathogenesis of this disease model. The role of macrophages in the anti-CD40 induced liver disease was demonstrated in previous studies [21, 24]. Inflammatory cytokines, especially TNFα and INFγ, and chemokine release from macrophages are believed to be the central mechanisms in development of necrotic liver damage and are well known to cause endothelial cell activation [24]. Therefore, we postulate that anti-CD40 activated macrophages cause TNFα and INFγ triggered endothelial cell activation, which can be reversed by heme. The fact that endothelial cells themselves express CD40 receptor, rises a second hypothesis that endothelial cells may as well get directly activated by anti-CD40 in the blood stream and that this activation can be supressed by heme priming [53].

Second, the mechanism behind the heme anti-inflammatory effect has still to be cleared and will be discussed in the following chapter.

6.2 Mechanisms involved in the suppressive effect of heme on the endothelial inflammatory response

Heme-driven hypoinflammation is Hmox-1 independent

Hmox-1, as one of the pivotal enzymes of anti-inflammation and anti-oxidation, is the major, rate-limiting enzyme in heme degradation [6]. To elucidate the dependence of heme-driven hypoinflammation on Hmox-1, we compared the role of heme in a LPS-induced inflammation mouse model in wild type and Hmox-1 knock-out animals. Interestingly, the heme-mediated suppressive effect on the endothelial inflammatory response in murine LuEC remained unchanged in Hmox-1 knock-out mice (Fig. 15) compared to the heme-mediated hypo-inflammatory effect on LuEC from wild-type mice (Fig. 10). Our results suggest that heme-dependent hmox-1 upregulation, which is described as the major protective anti-inflammatory and anti-oxidative cellular pathway [6], is not the main player driving the heme-dependent anti-inflammation observed.

Heme activates transcription factor Nrf2

To elucide the mechanism behind heme-driven hypoinflammation in endothelial cells, gene array experiments on HUVEC were conducted in our laboratory (data not shown). We observed heme-driven upregulation of Hmox-1, NQO1 and Scl7a11 genes, which share a common transcription factor Nrf2 [26]. Nrf2 is well known for its anti-oxidant and anti-inflammatory role and therefore we decided to investigate the involvement of Nrf2 in heme-driven hypoinflammation [27] .

First, we confirmed mRNA upregulation of the Nrf2 dependent genes NQO1, Scl7a11, GSR, and Hmox-1, and accumulation of Nrf2 protein in nuclear fractions of HUVEC upon heme stimulation (Fig. 16 and 17). Next, preliminary in vivo data on wild-type murine lung endothelial cells point to a tendency in heme-dependent mRNA upregulation of Nrf2 target genes Scl7a11 and Hmox-1 (Fig. 18). To reach statistical significance in these in vivo experiments with wide data point variance within a treatment group, further experiments with more animals are necessary. The dose-dependent upregulation of Nrf2 target genes in vitro and in vivo and the nucleic accumulation of Nrf2 protein upon heme-albumin treatment in vitro indicate a strong heme/Nrf2 interaction. To definitively proof the Nrf2 dependency of heme-mediated hypoinflammation, a Nrf2 knock-out model would be needed.

Further, the preserved supression of VCAM-1 expression by heme pre-stimulation in lung endothelial cells from Hmox-1 knock-out mice (Fig. 15) support the above mentioned theory of Kobayashi, that the Nrf2 anti-inflammatory effect is independent from its anti-oxidant pathway [9] and that heme acts via Nrf2 anti-inflammatory pathway independently from Hmox-1 .

6.3 Conclusions

Taken together, in this study we proved our hypothesis that heme causes suppression of inflammatory responses on endothelial cells. We showed heme-induced suppression of pro-inflammatory NFκB dependent adhesion molecules VCAM-1 and E-Selectin, and the chemokine IL-8. We could demonstrate for the first time that the suppressive effects on endothelial inflammation were related to heme itself and not to Hmox-1 expression. Furthermore, we could identify heme-mediated Nrf2 activation as a potential driver of hypoinflammation in endothelial cells.

7 References

1. Voet et al., Biochemistry, Wiley and sons, 2008.
2. Schaer, D.J. and P.W. Buehler, *Cell-free hemoglobin and its scavenger proteins: new disease models leading the way to targeted therapies.* Cold Spring Harb Perspect Med, 2013. **3**(6).
3. Rother, R.P., et al., *The clinical sequelae of intravascular hemolysis and extracellular plasma hemoglobin: a novel mechanism of human disease.* Jama, 2005. **293**(13): p. 1653-62.
4. Schaer, C.A., et al., *Mechanisms of haptoglobin protection against hemoglobin peroxidation triggered endothelial damage.* Cell Death Differ, 2013. **20**(11): p. 1569-79.
5. Schaer, D.J., et al., *Hemolysis and free hemoglobin revisited: exploring hemoglobin and hemin scavengers as a novel class of therapeutic proteins.* Blood, 2013. **121**(8): p. 1276-84.
6. Wagener, F.A., et al., *Heme is a potent inducer of inflammation in mice and is counteracted by heme oxygenase.* Blood, 2001. **98**(6): p. 1802-11.
7. Motterlini, R., B. Haas, and R. Foresti, *Emerging concepts on the anti-inflammatory actions of carbon monoxide-releasing molecules (CO-RMs).* Med Gas Res, 2012. **2**(1): p. 28.
8. Wegiel, B., et al., *Cell surface biliverdin reductase mediates biliverdin-induced anti-inflammatory effects via phosphatidylinositol 3-kinase and Akt.* J Biol Chem, 2009. **284**(32): p. 21369-78.
9. Jeney, V., et al., *Pro-oxidant and cytotoxic effects of circulating heme.* Blood, 2002. **100**(3): p. 879-87.
10. Belcher, J.D., et al., *Transgenic sickle mice have vascular inflammation.* Blood, 2003. **101**(10): p. 3953-9.
11. Wang, R., et al., *Stress-responsive heme oxygenase-1 isoenzyme participates in Toll-like receptor 4-induced inflammation during brain ischemia.* Neuroreport, 2016. **27**(6): p. 445-54.
12. Vallelian, F., et al., Revisiting the putative role of heme as a trigger of inflammation. Manuscript submitted
13. Kuzelova, K., M. Mrhalova, and Z. Hrkal, *Kinetics of heme interaction with heme-binding proteins: the effect of heme aggregation state.* Biochim Biophys Acta, 1997. **1336**(3): p. 497-501.
14. Khakpour, S., K. Wilhelmsen, and J. Hellman, *Vascular endothelial cell Toll-like receptor pathways in sepsis.* Innate Immun, 2015. **21**(8): p. 827-46.
15. Wilhelmsen, K., et al., *Activation of endothelial TLR2 by bacterial lipoprotein upregulates proteins specific for the neutrophil response.* Innate Immun, 2012. **18**(4): p. 602-16.
16. Ley, K., et al., *Getting to the site of inflammation: the leukocyte adhesion cascade updated.* Nat Rev Immunol, 2007. **7**(9): p. 678-89.
17. Fitzner, N., et al., *Human skin endothelial cells can express all 10 TLR genes and respond to respective ligands.* Clin Vaccine Immunol, 2008. **15**(1): p. 138-46.
18. Hickey, M.J. and P. Kubes, *Intravascular immunity: the host-pathogen encounter in blood vessels.* Nat Rev Immunol, 2009. **9**(5): p. 364-75.
19. Gerszten, R.E., et al., *MCP-1 and IL-8 trigger firm adhesion of monocytes to vascular endothelium under flow conditions.* Nature, 1999. **398**(6729): p. 718-23.
20. Collins, T., et al., *Transcriptional regulation of endothelial cell adhesion molecules: NF-kappa B and cytokine-inducible enhancers.* Faseb j, 1995. **9**(10): p. 899-909.
21. Kimura, K., et al., *Pivotal role of nuclear factor kappaB signaling in anti-CD40-induced liver injury in mice.* Hepatology, 2004. **40**(5): p. 1180-9.
22. Elgueta, R., et al., *Molecular mechanism and function of CD40/CD40L engagement in the immune system.* Immunol Rev, 2009. **229**(1): p. 152-72.
23. Wiley, J.A. and A.G. Harmsen, *Bone marrow-derived cells are required for the induction of a pulmonary inflammatory response mediated by CD40 ligation.* Am J Pathol, 1999. **154**(3): p. 919-26.

24. Kimura, K., et al., *Pathogenic role of B cells in anti-CD40-induced necroinflammatory liver disease.* Am J Pathol, 2006. **168**(3): p. 786-95.
25. Kimura, K., et al., *Activated intrahepatic antigen-presenting cells inhibit hepatitis B virus replication in the liver of transgenic mice.* J Immunol, 2002. **169**(9): p. 5188-95.
26. Thimmulappa, R.K., et al., *Nrf2-dependent protection from LPS induced inflammatory response and mortality by CDDO-Imidazolide.* Biochem Biophys Res Commun, 2006. **351**(4): p. 883-9.
27. Thimmulappa, R.K., et al., *Nrf2 is a critical regulator of the innate immune response and survival during experimental sepsis.* J Clin Invest, 2006. **116**(4): p. 984-95.
28. Itoh, K., et al., *Keap1 represses nuclear activation of antioxidant responsive elements by Nrf2 through binding to the amino-terminal Neh2 domain.* Genes Dev, 1999. **13**(1): p. 76-86.
29. Kobayashi, E.H., et al., *Nrf2 suppresses macrophage inflammatory response by blocking proinflammatory cytokine transcription.* Nat Commun, 2016. **7**: p. 11624.
30. Yu, Y., et al., *Fibroblast growth factor 21 (FGF21) inhibits macrophage-mediated inflammation by activating Nrf2 and suppressing the NF-kappaB signaling pathway.* Int Immunopharmacol, 2016. **38**: p. 144-52.
31. Ma, Q., *Role of nrf2 in oxidative stress and toxicity.* Annu Rev Pharmacol Toxicol, 2013. **53**: p. 401-26.
32. Okuda, Y., et al., *IL-6-deficient mice are resistant to the induction of experimental autoimmune encephalomyelitis provoked by myelin oligodendrocyte glycoprotein.* Int Immunol, 1998. **10**(5): p. 703-8.
33. Larsen, C.M., et al., *Sustained effects of interleukin-1 receptor antagonist treatment in type 2 diabetes.* Diabetes Care, 2009. **32**(9): p. 1663-8.
34. Yoh, K., et al., *Nrf2-deficient female mice develop lupus-like autoimmune nephritis.* Kidney Int, 2001. **60**(4): p. 1343-53.
35. Herrera, A., et al., *Staphylococcal beta-Toxin Modulates Human Aortic Endothelial Cell and Platelet Function through Sphingomyelinase and Biofilm Ligase Activities.* MBio, 2017. **8**(2).
36. https://www.licor.com/bio/applications/in-cell_western_assay/index.html
37. Instruction Manual, Bio-Plex Pro Human Inflammation Panel 1 (Bulletin 10044282) http://www.bio-rad.com/en-ch/product/human-inflammation-assays
38. Vallelian, F., et al., *Glucocorticoid treatment skews human monocyte differentiation into a hemoglobin-clearance phenotype with enhanced heme-iron recycling and antioxidant capacity.* Blood, 2010. **116**(24): p. 5347-56.
39. Schaer, D.J., et al., *CD163 is the macrophage scavenger receptor for native and chemically modified hemoglobins in the absence of haptoglobin.* Blood, 2006. **107**(1): p. 373-80.
40. Schmitz, B., et al., *Increased monocyte adhesion by endothelial expression of VCAM-1 missense variation in vitro.* Atherosclerosis, 2013. **230**(2): p. 185-90.
41. Skaria, T., E. Bachli, and G. Schoedon, *Wnt5A/Ryk signaling critically affects barrier function in human vascular endothelial cells.* Cell Adh Migr, 2017. **11**(1): p. 24-38.
42. Wang, R., et al., *The acute extracellular flux (XF) assay to assess compound effects on mitochondrial function.* J Biomol Screen, 2015. **20**(3): p. 422-9.
43. Agilent Seahorse XF Cell Mito Stress Test Kit User Guide, First edition, March 2017, Agilent Technologies, Wilmington, DE 19808-1610 USA
44. Agilent Seahorse XF Cell Mito Stress Test Kit User Guide, First edition, March 2017, Agilent Technologies, Wilmington, DE 19808-1610 USA
45. Bantikassegn, A., X. Song, and K. Politi, *Isolation of epithelial, endothelial, and immune cells from lungs of transgenic mice with oncogene-induced lung adenocarcinomas.* Am J Respir Cell Mol Biol, 2015. **52**(4): p. 409-17.
46. Lim, Y.C. and F.W. Luscinskas, *Isolation and culture of murine heart and lung endothelial cells for in vitro model systems.* Methods Mol Biol, 2006. **341**: p. 141-54.
47. Kensler, T.W., N. Wakabayashi, and S. Biswal, *Cell survival responses to environmental stresses via the Keap1-Nrf2-ARE pathway.* Annu Rev Pharmacol Toxicol, 2007. **47**: p. 89-116.

48. Iwasaki, K., et al., *Hemin-mediated regulation of an antioxidant-responsive element of the human ferritin H gene and role of Ref-1 during erythroid differentiation of K562 cells.* Mol Cell Biol, 2006. **26**(7): p. 2845-56.
49. Wagener, F.A., et al., *Heme induces the expression of adhesion molecules ICAM-1, VCAM-1, and E selectin in vascular endothelial cells.* Proc Soc Exp Biol Med, 1997. **216**(3): p. 456-63.
50. Figueiredo, R.T., et al., *Characterization of heme as activator of Toll-like receptor 4.* J Biol Chem, 2007. **282**(28): p. 20221-9.
51. Graca-Souza, A.V., et al., *Neutrophil activation by heme: implications for inflammatory processes.* Blood, 2002. **99**(11): p. 4160-5.
52. Barcellos-de-Souza, P., et al., *Heme modulates intestinal epithelial cell activation: involvement of NADPHox-derived ROS signaling.* Am J Physiol Cell Physiol, 2013. **304**(2): p. C170-9.
53. Pluvinet, R., et al., *CD40: an upstream master switch for endothelial cell activation uncovered by RNAi-coupled transcriptional profiling.* Blood, 2008. **112**(9): p. 3624-37.

8 Curriculum vitae

PERSONAL DATA

Name: Kristyna Valkova

Title: MD / Dr. med.

Date of birth: 25th March 1986

Place of origin: Wädenswil (ZH) and Czech Republic

EDUCATION

2000-2004	High School education at Kantonsschule Enge, Neusprachliches Gymnasium, Zurich
2004-2011	Medical School (Human Medicine), Faculty of Medicine, University of Zurich
2012	Doctorate in Human Medicine, University of Zurich
2012-2013	Clinical resident in Surgery, Zug Cantonal Hospital
2013-2015	Clinical resident in Internal Medicine, Zug Cantonal Hospital
2015-dato	Clinical resident in Internal Medicine and research associate, Department of Internal Medicine, University Hospital Zurich

9 Personal declaration

Name: Kristyna Valkova, MD

Matriculation number: 04-718-664

STATEMENT OF AUTHORSHIP

Hereby I declare that I have written the present master thesis independently under the sole aid of the sources mentioned in the reference list or aids as indicated. All passages quoted from publications or paraphrased from these sources are indicated as such, i.e. cited and/or attributed. This thesis was not submitted in any form for another degree or diploma at any university or other institution of tertiary education.

10 Acknowledgments

- I thank PD Dr. med. Florence Vallelian for giving me insights into the laboratory science, for the supervision of my master thesis and for her support in my clinical and research career
- I thank Prof. Dr. med. Dominik Schaer for giving me the opportunity to work in his research laboratory and for the supervision of my master thesis and my clinical work
- I thank Prof. Dr. Gabriele Schoedon for the revision of my master thesis and for teaching me basic laboratory techniques
- I thank Dr. Giada Ingoglia for sharing her enthusiasm and her knowledge in biology and biotechnology with me and for the daily support in the laboratory work
- I thank the laboratory members Dr. med. Christian Schaer, Msc; Dr. med. Jeremy Deuel, PhD and PD Dr. Rok Humar for their help, notably with technical questions
- I thank the laboratory technicians Nadja Schulthess and Kerstin Hansen for their help, especially during the busy period towards the end of my master thesis
- And last but not least, I want to thank my father Miloslav Kučera and my partner Gaudenz Halter, who encouraged and supported me along the way

In loving memory of my mother Alena